Improving ferrate disinfection and decontamination performance at neutral pH by activating peroxymonosulfate under solar light

Núria López-Vinent [abc1]****, Alberto Cruz-Alcalde*** [ab1]***, Gholamreza Moussavi*** [d]***, Isabel del Castillo Gonzalez*** [b]***, Aurelio Hernandez Lehmann*** [b]***, Jaime Giménez*** [a]***, Stefanos Giannakis*** [b]**

[a] *Department of Chemical Engineering and Analytical Chemistry, Faculty of Chemistry, University of Barcelona, C/Martí i Franqués 1, 08028 Barcelona, Spain.*

[b] *Universidad Politécnica de Madrid, E.T.S. de Ingenieros de Caminos, Canales y Puertos, Departamento de Ingeniería Civil: Hidráulica, Energía y Medio Ambiente, Unidad docente Ingeniería Sanitaria, C/Profesor Aranguren s/n, 28040 Madrid, Spain.*

c Department of Environmental Chemistry, IDAEA-CSIC, C/ Jordi Girona 18, 08034 Barcelona, Spain

[d] *Department of Environmental Health Engineering, Faculty of Medical Sciences, Tarbiat Modares University, Tehran, Iran*

***Corresponding author**: Núria López-Vinent (nuria.lopez@ub.edu)

****Corresponding author**: Stefanos Giannakis (Stefanos.Giannakis@upm.es)

[1] NLV and ACA have contributed equally to this work.

Abstract

In this work, the effect of solar light as a "reducing agent" in Fe(VI)/PMS process for disinfection and decontamination of water was investigated. Single, double and triple-factor disinfection processes were systematically studied against *Escherichia coli* and validated on sulfamethoxazole. The experiments performed with PMS or Fe(VI) in dark conditions only achieved 1-log reduction in 2 h, while no significant enhancement was found in the Fe(VI)/PMS system. The introduction of solar light in either PMS or Fe(VI) process enhanced the *E. coli* inactivation since complete inactivation (6-log) was reached at 90 min. However, the best improvement was done with the triple-factor disinfection process (Fe(VI)/PMS/solar light) which presented 6-log reduction at only 40 min. In the case of sulfamethoxazole, more than 70% removal was achieved under the Fe(VI)/PMS/solar light system, while only about 20% was observed with single and double-factor processes. Our study revealed the light spectrum distribution effects, the iron implications, while a main role for $HO^{\bullet}$ and the participation of $SO_4^{\bullet-}$ was found, without overlooking the direct effects of solar light and PMS itself, as well as the possible involvement of other transient species. Overall, the efficacy of the Fe(VI)/PMS/solar light process against a series of microorganisms combined with the effectiveness at near-neutral pH, suggest its suitability for further assessment in disinfection and/or decontamination of water.

Keywords: Solar disinfection (SODIS), Ferrate, Persulfate, *E. coli*, Radical oxidation, Water treatment

1. Introduction

Safe and readily available water is essential for public health if it is employed for drinking, domestic use, food production or recreational purposes. Enhanced water supply and sanitation, and better control of water resources can impulse the economic rise in countries. Additionally, it can take part in the poverty diminution, since clean water has been connected with health improvement and subsequently higher participation in lucrative activities [1]. It has been estimated that in 2017, 785 million people did not have access to basic drinking-water services and, globally, 2 billion people were consuming contaminated drinking water with feces [2]. The presence of pathogens in water causes water-related illness, including cholera, diarrhea, hepatitis A and polio, among others. It is estimated that 829 000 people die each year from diarrhea as a consequence of unreliable drinking-water, sanitation and lack of hands hygiene [2, 3]. Although these problems impact highly low-and-middle income countries, economically developed countries are not care-free; the presence of micropollutants (MPs), like pharmaceuticals, in water has increased the concern with water pollution since these are potentially toxic to human health and the environment [4, 5]. One of the measures established in the 6th Sustainable Development Goal was to guarantee available and sustainable management of water for all [6]. In this regard, the potential solutions to this problem should be safe and environmentally sustainable worldwide.

Although various physical and chemical methods have been evaluated for contaminated water disinfection, chlorination is the most accepted method of disinfecting the contaminated waters. The main drawback of the chlorination is the formation of toxic disinfection by-products (DBPs), such as trihalomethanes, from the reaction between chlorine and natural organic matter precursors present in water [7]. Therefore, DBPs are generally of high concern for the public health because they could be dangerous for human health and the aquatic ecosystems [8].

Advanced oxidation processes (AOPs) as a new class of water treatment methods have been shown very efficient for the disinfection along with the organic micropollutants degradation [9-12]. The iron-

based AOPs are among the investigated ones for disinfection and decontamination [3, 13-15]. Ferrate (Fe(VI)), a high-valent form of iron, has been long known in environmental processes such as remediation and water treatment, because of its potential in multifunctional processes (i.e., oxidation, coagulation, and disinfection). Fe(VI) is highly reactive with organic compounds which content nitrogen, sulfur and moieties with unsaturated bonds and aromatic rings. Additionally, the subsequent reactions of Fe(VI) would form nano-sized particles, like ferric oxides/hydroxides, which could facilitate water coagulation [16-18]. Some studies have demonstrated the efficiency of Fe(VI) in the disinfection of viruses and bacteria, such as MS2 bacteriophage [19] and *Escherichia coli* [20]. As well as in the oxidation of a wide range of MPs, like sulfamethoxazole, enrofloxacin, carbamazepine, diclofenac, atrazine, ibuprofen, naproxen, between others [21-24]. However, an inherent drawback of Fe(VI) is its chemical instability, due to its fast reduction in water, both in acidic and neutral conditions (Eq. 1 and Eq. 2).

$$4FeO_4^{2-} + 20H^+ \rightarrow 4Fe^{3+} + 10H_2O + 3O_2 \quad \text{(Eq.1)}$$

$$4FeO_4^{2-} + 10H_2O \rightarrow 4Fe^{3+} + 20OH^- + 3O_2 \quad \text{(Eq.2)}$$

Because of this intrinsic property of ferrate, a solution to enhance the efficiency of the process prolonging the oxidation is needed [25]. Previous works investigated the combination of ferrate and peroxymonosulfate (PMS), which is also an oxidant but acts either as electron acceptor or donor, to improve the degradation of different MPs [25-27]. Fe(III) generated in reaction 1 could activate PMS, forming peroxymonosulfate radical (which is mildly oxidative and may assist in disinfection [28, 29]) Fe(II), while the latter can further react with peroxymonosulfate to generate sulfate radical ($SO_4^{\bullet -}$) by reactions Eq.3 and Eq.4.

$$HSO_5^- + Fe^{3+} \rightarrow Fe^{2+} + SO_5^{\bullet -} + H^+ \quad \text{(Eq.3)}$$

$$HSO_5^- + Fe^{2+} \rightarrow Fe^{3+} + SO_4^{\bullet -} + OH^- \quad k = 3.0 \times 10^4\ M^{-1}\ s^{-1} \quad \text{(Eq.4)}$$

Feng et al. [26] reported that although addition of PMS to the reaction medium enhanced the oxidation of fluoroquinolones by Fe(VI), the removal efficiency at the end of the treatment was still below 60%.

It was due likely to the slow reduction of Fe(III)to Fe(II) shown in Eq.3, resulting in a low generation of $SO_4^{\bullet-}$ (Eq. 4) [25, 30]. To address this defect, the effect of different reducing agents, such as hydroxylamine, ascorbic acid and sodium thiosulfate, has been investigated for the acceleration of the reduction of Fe(III) to Fe(II). The findings revealed that the degradation of the selected contaminants improved when the reducing agents were added to the Fe(VI)/persulfate process [25, 31].

Nevertheless, the addition of reductants to an AOP may act in an antagonistic way; Fe(VI) can be reduced before exerting its oxidation action; thus the overall enhancement of the treatment process could be attributed to the generation of other reactive species, e.g. reaction of lower valence iron with the added oxidants. For instance, Rodriguez-Chueca et al. [32] investigated Fe(II)/Fe(III) to activate sulfite, a reductant, in order to generate $SO_3^{\bullet-}, SO_4^{\bullet-}$ and $HO^{\bullet}$. There are, however, other alternatives such as light irradiation to maintain a higher activity in the PMS/ Fe(VI) without hampering the Fe(VI) contribution. For instance, in the photo-Fenton process, photo-active Fe(III)-aqua-complexes can be reduced to Fe(II) by the action of solar light, in kinetics much higher than the reduction of Fe(III) to Fe(II) by H_2O_2 [33]. Hence using solar light might be an interesting option, supported by the following facts:

i) Solar light contains a small fraction of UVB wavelengths, which however could cause photolysis of MPs [34], activate PMS to generate $SO_4^{\bullet-}$ and $HO^{\bullet}$ [35], or directly damage microorganisms' genetic material [36],

ii) UVA light is present x10 more than UVB, and initiates germicidal, intracellular, auto-catalytic photo-Fenton reactions in bacteria [37], assists in Fe(III) to Fe(II) cycling [38] as well as impulses effective synergies with PMS [35].

iii) Visible light, on the other hand, constitutes the major fraction of solar light, which is a potentially exploitable resource, since PMS-Fe complexes have been shown to present higher activation and radical species' generation [39] (PMS in normal μM-mM concentrations is not activated by vis light, due to its absorption by Fe) [40].

To the best of the authors' knowledge based on the available published literature, there are no studies investigating the effect of solar light as a "reducing agent" in the Fe(VI)/PMS process towards the enhancement of the disinfection and/or the decontamination of water. Therefore, this work was aimed at investigating the effect of Fe(VI)/ solar light photocatalytic activation of PMS for the disinfection of water, using one of the few (if not the only) commercially available Fe(VI) product in Europe, ENVIFER (NANO IRON, s.r.o, Czechia).

Accordingly, in this work, the effectiveness of PMS and Fe(VI) combined with solar light was assessed on its disinfection and decontamination efficacy at neutral pH. More specifically, the single, double and triple-factor disinfection processes were systematically studied against *Escherichia coli* (as a model of bacterial pathogens) and validated on Sulfamethoxazole (as a model of MP, a recalcitrant antibiotic). Furthermore, we delineated the performance of this process on *Escherichia coli* inactivation by scrutinizing the operational parameters involved, such as different pH levels (from 5.5 to 8.5), the effect of different light wavelengths (solar light, UVA and UVB) and oxidants, i.e., peroxymonosulfate (Oxone^{TM}-PMS), sodium persulfate (PDS) and hydrogen peroxide (H_2O_2). We expanded the inactivation capacity of the combined processes towards various microorganisms (wild *Escherichia coli* isolates, vegetative *Bacillus subtilis* cells, *Raoutella planticola* as a *Klebsiella* surrogate, wild *Enterococcus sp.* isolates as a gram-Positive model bacteria and the *Saccharomyces cerevisiae* yeast, as a eukaryotic microorganism. Finally, based on the experimental results of cell protein and membrane oxidation assays, and a bio-compatible scavenger study, we propose an integrated proposal for the events taking place and a postulate mechanistic interpretation of bacterial disinfection under the combined Fe(VI)/PMS/solar light process.

2. Materials and methods

2.1. Chemical and reagents

Sulfamethoxazole (Merck, Spain) was used as a target compound. Potassium ferrate - Fe(VI) (29%, ENVIFER, NANO IRON, s.r.o., Czechia), potassium peroxymonosulfate (Oxone^{TM}; Merck, Spain), sodium persulfate (NaS_2O_8; Merck, Spain) and hydrogen peroxide (H_2O_2 30% w/v; Merck, Spain) were used as oxidant. Ferrozine ($C_{20}H_{13}N_4NaO_6S_2$ x H_2O; Merck, Spain), ammonium acetate ($CH_3CO_2NH_4$; Merck, Spain), ammonium hydroxide (NH_4OH 28-30%; Merck, Spain), hydroxylamine hydrochloride (NH_2OH x HCl; Merck, Spain), iron chloride ($FeCl_3$; Panreac, Spain) and hydrochloric acid (65% HCl, Merck, Spain) were used to analyze Fe(II) and Fe(III). Sodium bicarbonate ($NaHCO_3$; Merck, Spain) and potassium iodide (KI; Merck, Spain) were employed to analyze PMS. Acetonitrile (C_2H_3N; Panreac, Spain) and ortophosphoric acid (H_3PO_4; Panreac, Spain) were used for the mobile phase in High Performance Liquid Chromatography (HPLC) analyses. Methanol (MeOH; Panreac, Spain), deuterium oxide (D_2O; Merck, Spain), tert-butanol (tBuOH; Panreac, Spain) and nitrogen (N_2; Messer Iberica Gases) were used in the radical scavenger tests. Thiobarbituric acid ($C_4H_4N_2O_2S$, TBA; Merck, Spain), malondialdehyde tetrabutylammonium salt ($C_{19}H_{39}NO_2$ 96%; Merck, Spain) and glacial acetic acid (CH_3COOH; Merck, Spain) were used to analyze malondialdehyde MDA generation. Finally, the Bradford solution for protein determination (Panreac, Spain), albumin crude from chicken egg (Panreac, Spain), Tris-hydrochloride for buffer solutions (Panreac, Spain), potassium phosphate mono- and di-basic (KH_2PO_4 and K_2HPO_4; Merck, Spain) were employed for protein experiments.

2.2. Experimental setup

All experiments were carried out in a bench-scale solar simulator (SUNTEST CPS, Heraeus) with artificial sunlight provided by a 1500-W Xenon lamp equipped with both infrared and 290 nm cut-off filters. During entire experiment the system was air-cooled. The irradiance was set at 550 W m^{-2} and

monitored by a pyranometer (CM6b, Kipp & Zonen), which was located at the end of the solar simulator chamber in order to control the irradiance during the entire experiment.

UVB and UVA irradiation were facilitated by fluorescent TLD-type lamps (Philips), in a metallic housing. Specifically, the UVB was emitted by an array of 20-W TL-D 01 lamps with a narrow emission spectrum, centered on around 313 nm. The UVA irradiation was supplied by 18-W TL-D BLB lamps, with the emission peak found at 365 nm (the spectra for the Xe, UVB and UVA lamps can be found in the Supplementary Material, Figures S1-S3).

To perform the experiments, cylindrical Pyrex glass reactors (diameter 6 cm, height 9 cm, volume: 50 mL) were used under constant stirring (350 rpm). Temperature never exceeded 35 ºC and pH was 6.5 unless stated otherwise (*i.e.*, pH investigation). After each experiment the reactors were washed with ethanol, nitric acid and demineralized water to remove any organic contaminant as well as iron residues. Finally, the reactors were also sterilized by autoclaving (AUTESTER-P, SELECTA, Spain).

2.3. Bacterial preparation and enumeration protocols

The experiments of bacterial inactivation were carried out using a wild-type *Escherichia coli* strain K12, acquired from the German Collection of Microorganisms and Cell Cultures GmbH (DSM 498). This strain is non-pathogenic and allows as good approximation of wild-type *E. coli* (the most common indicator for enteric pathogens). *E. coli* was stored in cryo-vials with 20% glycerol at -80ºC, while working stocks remained at -80ºC. For comparison purposes, *Bacillus subtilis* (vegetative cells, DSM 10), *Raoutella planticola (ex-Klebsiella planticola* or *Klebsiella trevisanii*, DSM 3069), *Saccharomyces cerevisiae* (DSM 70449), plus two wastewater isolates (*E. coli* and *Enterococcus sp.*) were also used as bacterial models in this investigation [41].

To prepare the bacterial stock, LB medium was inoculated and was incubated at 37 ºC (for *E. coli* and *Enterococcus sp.*), 30 ºC (*B. subtilis* and *R. planticola*), or 25 ºC (in YPD medium for *S. cerevisiae*), and aerobically agitated at 180 rpm, overnight. Then 1 mL of that suspension was centrifuged during

2 min at ×8000 rpm. At this time the supernatant growth medium was withdrawn from the tube and the pellet formed was washed with sterile isotonic saline solution (8 g NaCl L^{-1} and 0.8 g KCl L^{-1}). The final stock corresponds to around 10^9 CFU mL^{-1} and was diluted down to create the working solution for the experiments, at 10^6 CFU mL^{-1}. The detailed procedure can be found elsewhere [2, 7]. To follow the evolution of bacterial population versus time, 100 μL samples were withdrawn from the photoreactor during the experiment and spread on Petri dished containing non-selective media. When necessary, samples were diluted (1:10) in saline solution to assure measurable counts of colonies (between 15-150 colonies per plate). After 24 h incubation at 37 ºC for *E. coli, B. subtilis* and *R. planticola,* and 48 h at 30 ºC for *S. cerevisiae* and *Enterococcus,* colony forming units were manually counted (detection limit 10 CFU mL^{-1}).

2.4. Analytical Methods

2.4.1. Micropollutant's evaluation

High Performance Liquid Chromatography (HPLC) by a Shimadzu LC-10A equipment was employed to measure the concentration of Sulfamethoxazole (SMX) against time. An isocratic method was used with acetonitrile and water acidified with ortophosphoric acid (pH=3) with a vol.% ratio of 20:80, respectively, as mobile phase. C-18 column (Supelco, 250 x 4.6 mm i.d; 5 μm particle size) was used and the detection wavelength was fixed at 270 nm. The flow was set at 1 mL min^{-1} and an injection of 100 μL was used.

2.4.2. Oxidants' determination

The concentration of PMS during the experiment was followed by the methodology proposed by Waclawek and coworkers [42]. This method uses a stock solution of KI (100 g L^{-1} mixed with 5 g L^{-1} of $NaHCO_3$ to avoid the oxidation of KI by O_2). In brief, to analyze the active part of PMS from Oxone™ 1 mL of sample was mixed with 100 μL of KI's stock solution and measured in the

210 spectrophotometer at 395 nm. In the text, whenever PMS addition is mentioned, we refer to the amount
211 of Oxone^{TM} added, if not specified otherwise.
212 Following the guidelines of the manufacturer (safety data sheet and standard operation practice
213 manual) and an initial optimization investigation, the stock solution of ferrate was freshly prepared
214 before experimentation by adding 1 g of potassium ferrate in 500 mL of demineralized water at 4 ºC
215 and pH= 9 (optimal conditions to obtain a stable solution of potassium ferrate), was used immediately
216 and discarded. The quantification of ferrate was determined by direct analyses in spectrophotometer
217 (VR-2000, SELECTA, Spain) as proposed by Y.L. Wei et al. [43], but at 510 nm, which provides the
218 sum of Fe(V)/ Fe(VI). In the text, whenever the addition of Fe(VI) is mentioned, we refer to the
219 amount of ENVIFER added (29% Fe(VI)). Finally, the Fe(III) and Fe(II) concentrations were
220 analyzed using the spectrophotometric ferrozine method suggested by Viollier and coworkers [44] and
221 quantified over pre-made calibration curves from Fe standards.
222 *2.4.3. Protein analyses (Bradford assay)*
223 To quantify the protein concentration in (total) cell lysates, albumin from chicken egg was used as a
224 standard. The standard was diluted such that the final concentrations are 0, 2.5, 5, 7.5, 10 and 12.5 μg
225 mL^{-1} in 0.5 mL of 50mM Tris buffer (pH 8.0). The protein sample was diluted 500-fold to a final
226 volume of 0.5 mL. To the standard and protein samples, 0.5 mL of Bradford solution was added, and
227 the absorbance was measured at OD_{595} after 10 min [45].
228 In order to analyze the intracellular proteins, KPi and Tris-EDTA reagents were added to the sample
229 before sonicating (UP200S, Hielscher) the sample at 4 ºC (on ice) during 15 min at 100% amplitude
230 in 0.5 s cycles to break the bacterial wall. Then, the sample was centrifuged at ×12000 rpm for 15 min
231 (MiniSpin, Eppendorf) and the supernatant was analyzed to obtain the intracellular protein.
232 The cell wall lipid peroxidation was determined by measuring the MDA formation, during the
233 experiments, following the methodology proposed by Zeb and Ullah [46]. In order to obtain a
234 measurable MDA concentration, these analyses were performed by experiments with 10^8 CFU mL^{-1}.

3. Results and discussion

3.1. Single factor disinfection tests

The inactivation efficiency of *E. coli* was tested in dark conditions at a (max.) temperature of 35 ºC and pH=6.5, as control test. The results revealed no differences on *E. coli* population along 3 h. Ferrate, solar light (SODIS) and PMS were then evaluated separately to investigate the potential inactivation of *E. coli* (10^6 CFU mL^{-1}) by each one of these factors. The results of *E. coli* inactivation by PMS and Fe(VI) are depicted in Fig. 1a and b, respectively.

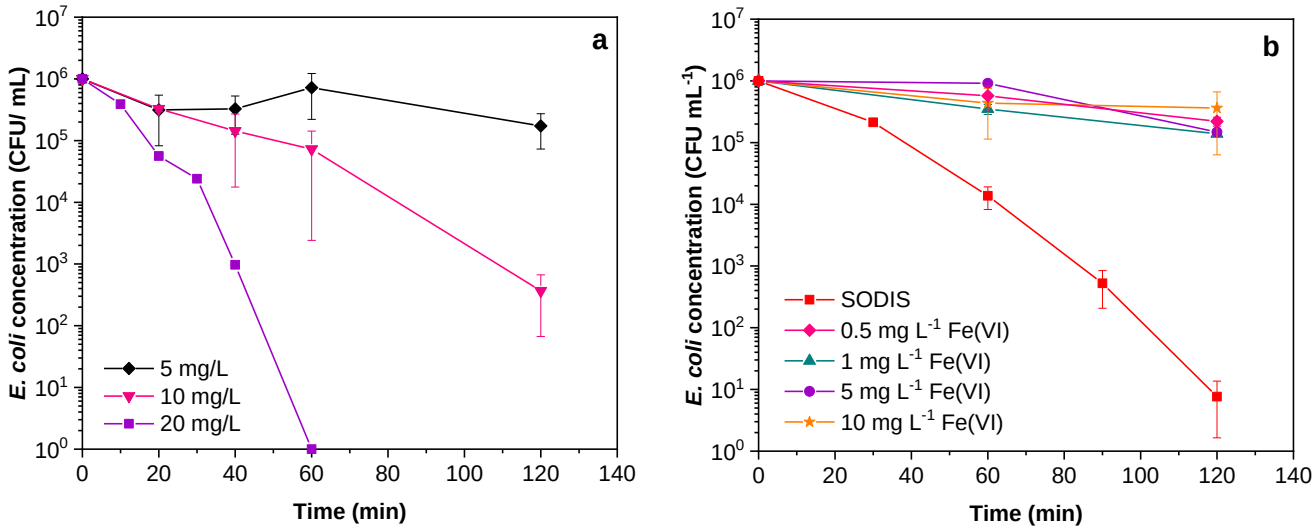

Figure 1. a) Single factor E. coli inactivation by PMS (5, 10 and 20 mg L^{-1}) and b) by Fe(VI) (0.5, 1, 5 and 10 mg L^{-1}) in dark conditions and solar light alone (solar irradiance: 550 W m^{-2}); T= 35 ºC; pH= 6.5.

As can be observed in Fig. 1a, three concentrations of PMS were used (5, 10 and 20 mg L^{-1}) in dark conditions and pH=6.5. The experiments using the highest concentration of PMS achieved total inactivation of *E. coli* in 60 min, while with the lowest one less than 1 log-inactivation was observed (1.7×10^5 CFU mL^{-1}). The apparent fluctuation is negligible (see SD expressed by the vertical bars) and intrinsic of the plate count method. For the tests performed with 10 mg L^{-1} of PMS about 3.5 log

254 reduction was seen at the end of the treatment (3.6 x 10^2 CFU mL^{-1}). It is found from the results shown
255 in Fig. 1a that PMS is able to inactivate *E. coli* by itself, but relatively high concentration of PMS and
256 time of contact are required. At this temperature, no PMS activation is assumed to generate sulfate and
257 hydroxyl radicals [47] thus the inactivation is a result of direct oxidation; the inactivation mechanism
258 is a consequence of the PMS and bacterial membrane redox potential (2.01 V [48] and 0.7 V [49, 50],
259 respectively). However, these concentrations of PMS would result in high residual sulfate ions in a
260 potential application (theoretical stoichiometry: 1 mole Oxone^{TM} = 4 moles of sulfates), hence its direct
261 use is not recommended, and its activation may result in lower amounts necessary.
262 Following, from the results of the experiments using Fe(VI) in dark conditions (Fig. 1b) it can be
263 observed that no significant differences in *E. coli* inactivation was seen by the different concentrations
264 used (0.5, 1, 5 and 10 mg L^{-1}) and pH=6.5. In all cases, the reduction of *E. coli* population was lower
265 than 1 log. This fact can be attributed firstly to the fact that ENVIFER contains 29% Fe(VI), which
266 makes higher concentrations compete with the other Fe forms in the salt. Also, there is rapid reduction
267 of Fe(VI) to Fe(III) by water due to the higher concentration of Fe(VI) compared to the other
268 experiments. Additionally, since the pH of the tests was 6.5, the formation of iron oxo-hydroxides
269 could diminish the inactivation of *E. coli*.
270 Finally, SODIS was also performed using a solar simulator at a fixed irradiance (550 W m^{-2}). In that
271 case, about 5-log inactivation of *E. coli* was achieved at 120 min. Solar light has the potential to
272 inactivate bacteria via the actions of the different light wavelengths emitted. UVB can directly damage
273 the bacterial genome, while UVA can initiate intracellular photocatalytic reactions, which lead to cell
274 death; since this is only a baseline process, the solar inactivation mechanisms will not be addressed
275 anew; interested readers should refer to [41].

276 ***3.2. Two-factor disinfection process***

277 The lack of disinfection effect of Fe(VI) by itself at the concentrations tested in this study, as well as
278 the requirement of a high reaction time (2.5 h) to inactivate *E. coli* under solar light and the necessity

of high concentrations of PMS to show adequate log-reductions of bacterial concentration, evidences the requirement of activator agents to enhance the efficiency of the process. Hence, the activation of PMS by Fe(VI) or solar light, and the Fe(VI)/ solar light processes were investigated. The results are given in Fig. 2a and b..

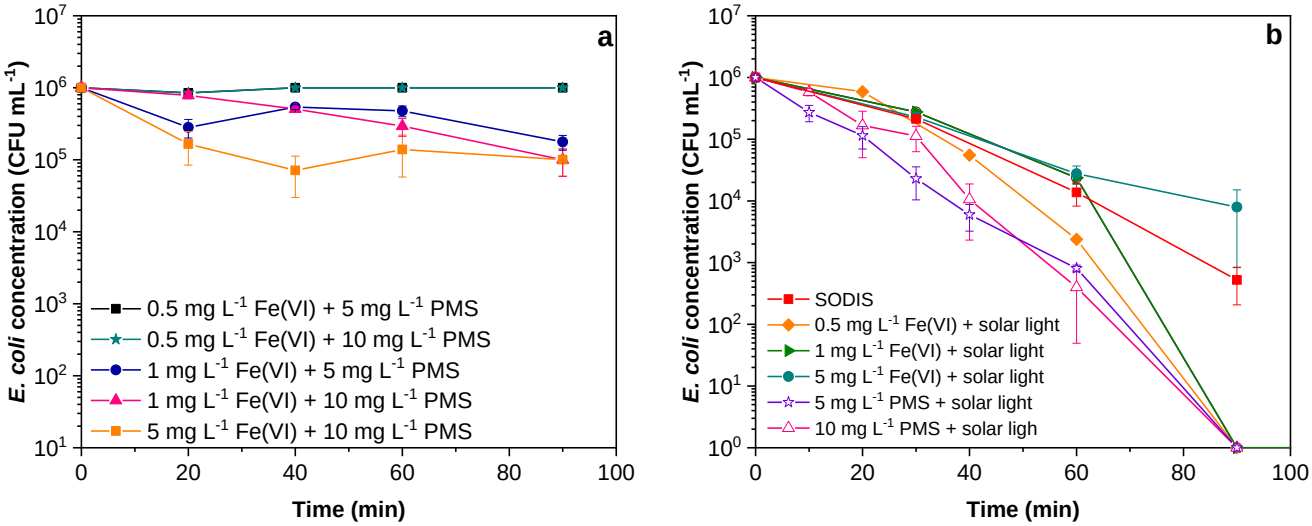

Figure 2. Double factor E. coli inactivation a) by Fe(VI) (0.5, 1 and 5 mg L^{-1}) PMS (5 and 10 mg L^{-1}) in dark conditions, and b) simulated solar light (irradiance: 550 W m^{-2}) with 5 and 10 mg L^{-1} of PMS, solar light/Fe(VI) (0.5, 1 and 5 mg L^{-1}) and solar disinfection (SODIS); T= 35 ºC; pH= 6.5.

In order to compare the *E. coli* reduction under diverse agents, the pseudo first-order kinetics (k, min^{-1}) were estimated by linear regression fitting the inactivation curves to pseudo-first order kinetics (see Supplementary material Table S1). The investigation of the synergistic or antagonistic effects when mixing the involved agents was performed on the basis of experimentally obtained kinetic constants and subsequent calculations of corresponding effects [51, 52], according to the Eqs. (5-7).

$$S_{\frac{Fe(VI)}{PMS}} = \frac{k_{\frac{Fe(VI)}{PMS}}}{k_{Fe(VI)}+k_{PMS}} \quad \text{(Eq.5)}$$

297 $$S_{\frac{PMS}{solar}} = \frac{k_{\frac{PMS}{solar}}}{k_{PMS}+k_{solar}}$$ (Eq.6)

298 $$S_{\frac{Fe(VI)}{solar}} = \frac{k_{\frac{Fe(VI)}{solar}}}{k_{Fe(VI)}+k_{solar}}$$ (Eq.7)

299 From the results observed in Fig. 2a, it seems that the addition of Fe(VI) to activate PMS did not
300 improve the process thus no synergy was found under the selected conditions. For instance, the
301 calculated factor for 5 mg L^{-1} of PMS and 1 mg L^{-1} of Fe(VI) was equal to $S_{Fe(VI)/PMS}$= 0.43, even
302 suggesting antagonistic effects. This phenomenon could be related to the inefficient PMS activation
303 by an oxidant that leads to the generation of peroxymonosulfate radical (Eq.3). This radical has lower
304 oxidation potential than sulfate or hydroxyl radical (i.e., only 1.1 eV, compared to 2.5 and 2.8 eV) and
305 does not lead to the same inactivation efficacy. Its implications in a reaction cascade that involves the
306 generation of further oxidative species (Eq. 8 and Eq. 9) has been proven [53, 54], however it appears
307 that when bacteria are used as an evaluation target, the effect seems relatively modest due to
308 peroxymonosulfate radical's low oxidative potential .

309 $$2SO_5^{\bullet -} + H_2O \rightarrow 2HSO_5^- + {}^1O_2$$ (Eq.8)

310 $$2SO_5^{\bullet -} \rightarrow S_2O_8^{2-} + O_2$$ (Eq.9)

311 Furthermore, as also previously encountered in literature [55], the subsequent reduction of Fe(III) to
312 Fe(II) is low, and limits the effective PMS activation. Hence, this limitation, that led previous works
313 to look for additives to enhance the reduction, has also appeared in this work.

314 Concerning the results of Fe(VI) combination with light (Fig. 2b), differences can be observed
315 depending on the employed oxidant concentration. For instance, an antagonistic effect ($S_{Fe(VI)/solar\ light}$=
316 0.49) was observed with the highest concentration of Fe(VI) (5 mg L^{-1}). This fact could be associated
317 to the higher kinetics in the generation of iron hydroxides when high Fe(VI) concentrations are used,
318 decreasing the efficiency of the process due to light scattering (coloring of solution is visibly noted).
319 Nevertheless, in the experiments with lower concentration of Fe(VI) a synergy is observed. The
320 calculated factor was $S_{Fe(VI)/solar\ light}$ = 1.13 and 1.16 for, 0.5 and 1 mg L^{-1} of Fe(VI), respectively. In

these cases, total bacterial inactivation was achieved at 1.5 h, while less than 1 log-reduction took place without light and less than 3.5 log-inactivation was observed under light exposure at the same time. Here, light scattering effects are less probable when operating at these conditions, which permits the un-interrupted direct solar light action to take place. Concerning the mechanism of Fe(VI)/solar light, it could be elucidated by previous reactions (Eq.1 and Eq.2) and, after its reduction to Fe(III), the following one (Eq.10).

$$Fe^{3+} + H_2O \xrightarrow{hv} Fe^{2+} + H^+ + HO^{\bullet} \quad \text{(Eq.10)}$$

Hence, an effective reduction of Fe(III) by light generates hydroxyl radicals which could participate in the inactivation of *E. coli*, enhancing the process efficiency as explained above. Considering that the Fe(VI) will eventually lead to ferric (hydr)oxides, and these positive particles may in turn attach to the bacterial wall, further oxidative events may be occurring: the presence of iron has been proven to lead an effective ligand-to-metal charge transfer (LMCT) between iron-bacterial cell wall components complex (e.g., carboxylic acids) [56].

$$[Fe(COO-R)]^{2+} + hv \rightarrow Fe^{2+} + CO_2 + R^{\bullet} \quad \text{(Eq.11)}$$

The process is effectuated via the cell wall as a sacrificial electron donor, damaging the cell integrity while generating Fe(II) which in turn enhances the intracellular Fe(II) diffusion that enhances the photo-Fenton processes taking place under light [51, 57].

Finally, in the activation of PMS by solar light [3] a similar behavior to that for the Fe(VI)/PMS process was observed with high PMS concentrations. However, this effect was less noticeable compared to the previous case. The results are also depicted in Fig. 2b. The case in which 10 mg L^{-1} of PMS was applied, although the value of k_{obs} was higher in the PMS/solar light process (0.16 min^{-1}) compared to the single PMS condition (0.07 min^{-1}) or solar light alone (0.09 min^{-1}), the calculated factor was $S_{PMS/solar\ light}$= 1. This indicates that there was no synergy in that combination. Possibly, these results could be attributed to a competition between *E. coli* and PMS for photons. On the other hand, the production of more $SO_4^{\bullet-}$ or $HO^{\bullet}$, with increasing PMS concentrations leads to higher

radicals' production; this excess of $SO_4^{\bullet -}$ or $HO^{\bullet}$, can attack cells, but could react with themselves or PMS (reaction 8 and 9), decreasing the efficiency of the process [58]. In sum, Eqs. 12-20 [59-61] describe the radical production ($SO_4^{\bullet -}$, $SO_5^{\bullet -}$, $\frac{HO_2^{\bullet}}{O_2^{\bullet -}}$, and $HO^{\bullet}$), which have demonstrated inactivation efficacy.

$$HSO_5^- \xrightarrow{h\nu} SO_4^{\bullet -} + HO^{\bullet} \quad \text{(Eq. 12)}$$

Sulfate radical involvement:

$$SO_4^{\bullet -} + H_2O \rightarrow + HSO_4^- + HO^{\bullet} \quad k = 660\ s^{-1} \quad \text{(Eq. 13)}$$

$$SO_4^{\bullet -} + OH^- \rightarrow SO_4^{2-} + HO^{\bullet} \quad k = 7 \cdot 10^7\ M^{-1}\ s^{-1} \quad \text{(Eq. 14)}$$

$$SO_4^{\bullet -} + SO_4^{\bullet -} \rightarrow S_2O_8^{2-} \quad k = 4 \cdot 10^8\ M^{-1}\ s^{-1} \quad \text{(Eq. 15)}$$

$$SO_4^{\bullet -} + HSO_5^- \rightarrow SO_5^{\bullet -} + HSO_4^- \quad k = 1 \cdot 10^6\ M^{-1}\ s^{-1} \quad \text{(Eq. 16)}$$

Hydroxyl radical involvement:

$$HO^{\bullet} + HSO_5^- \rightarrow SO_5^{\bullet -} + H_2O \quad k = 1.7 \times 10^7\ M^{-1}\ s^{-1} \quad \text{(Eq. 17)}$$

$$HO^{\bullet} + HO^{\bullet} \rightarrow H_2O_2 \quad k = 5.5 \times 10^9\ M^{-1} \cdot s^{-1} \quad \text{(Eq. 18)}$$

$$HO^{\bullet} + H_2O_2 \rightarrow HO_2^{\bullet} + H_2O \quad k = 2.7 \times 10^7\ M^{-1}\ s^{-1} \quad \text{(Eq. 19)}$$

$$HO_2^{\bullet} \Leftrightarrow O_2^{\bullet -} + H^+ \quad pKa = 4.88 \quad \text{(Eq. 20)}$$

In the same process but using 5 mg L^{-1} of PMS instead, the calculated factor was $S_{PMS/solar\ light}$=1.35. This suggests that the existence of a synergistic effect strongly depends on the oxidant concentration. Additionally, the results of PMS/solar light with two PMS concentrations were very close during entire experiment, which corroborates the explanation about the differences between the abovementioned PMS concentrations. An important fact to consider is the generation of $HO^{\bullet}$, which reacts 10 times faster with biomolecules compared to sulfate radicals [3, 62]. This fact could be a possible explanation to the observed process improvement.

3.3. Three-factor disinfection in the Fe(VI)/ PMS/solar light combined process

Since the performance of double factor bacterial inactivation was tested and the disinfection was not always effective, the combination of the three factors was investigated to search for a more efficient process. The employed Fe(VI) and PMS concentrations were 1 and 5 mg L^{-1}, respectively. These concentrations were selected since in the single and double factor inactivation tests the inactivation rate of *E. coli* was modest, and therefore any multi-factor synergy under these conditions was expected to be more clearly observed. In this phase of the work, after bacteria the performance of PMS, Fe(VI) and sunlight irradiation process was investigated for both bacterial inactivation and antibiotic SMX degradation and the results are shown in Fig. 3.

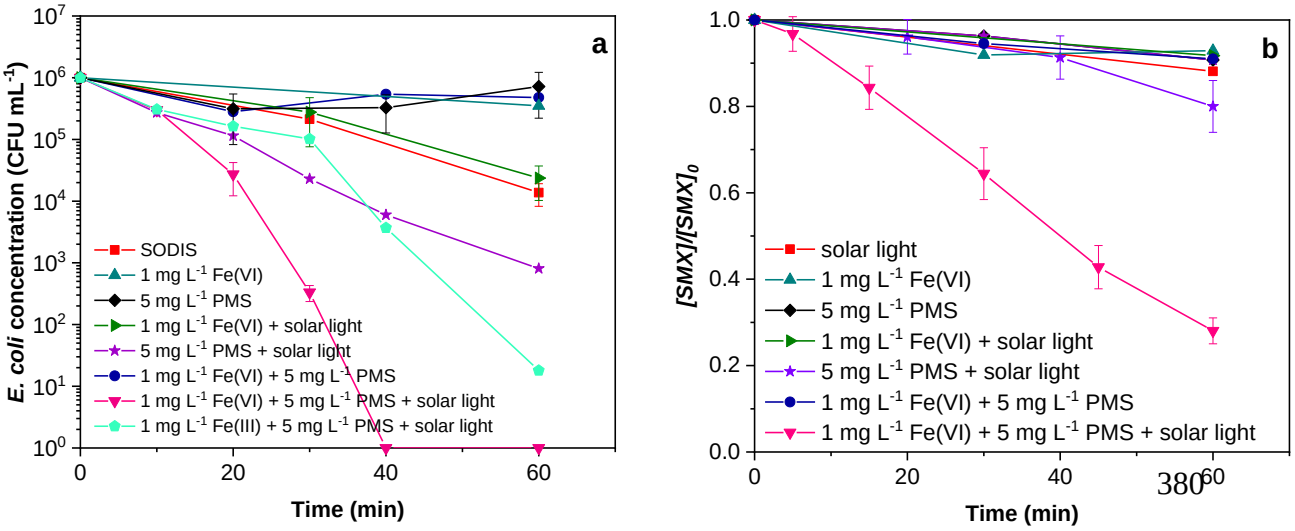

Figure 3. Performance of coupling Fe(VI), PMS and solar light irradiation to a) inactivate E. coli, and b) remove sulfamethoxazole (0.1 mg L^{-1}); [Fe(VI)]= 1 mg L^{-1}; [PMS]= 5 mg L^{-1} and solar irradiance: 550 W m^{-2}; T= 35 ºC; pH= 6.5.

As a baseline event, in dark conditions using Fe(VI), PMS and the mixture of both, poor performances were obtained in the *E. coli* reduction, as explained in sections 3.1 and 3.2. When light was introduced

388 in the process containing either PMS or Fe(VI), a relative improvement in the disinfection performance
389 was observed (Fig. 3a). When the three factors were combined (Fe(VI)/PMS/solar light process), the
390 *E. coli* inactivation was significantly enhanced, compared to the other tests. Total bacterial inactivation
391 was achieved in only 40 min, reducing the total treatment time by 65% compared to PMS/solar light
392 or Fe(VI)/solar light processes. When combining all three constituents (Fe(VI)/PMS/solar light), the
393 synergy factor was calculated to be $S_{Fe(VI)/PMS/solar\ light}$= 2.03 (Eq.21), indicating a clear synergy in this
394 combined process (k constants available at the Supplementary material Table S1).

395 $$S_{\frac{Fe(VI)}{\frac{PMS}{solar}}} = \frac{k_{Fe(VI)/PMS/solar}}{k_{Fe(VI)}+k_{PMS}+k_{solar}} \quad \text{(Eq.21)}$$

396 This improvement in bacterial reduction could be explained by the previous reactions (Eq.1- Eq.10).
397 However, the most important one is presumably the reduction of Fe(III) to Fe(II) (Eq.10) after Fe(VI)
398 reaction with bacteria or PMS, which could then react with PMS yielding more $SO_4^{\bullet-}$ (Eq.4),
399 intracellular events, side-reactions with the generated H_2O_2 and $S_2O_8^{2-}$, leading to an overall
400 enhancement of the process.

401 $$Fe^{2+} + H_2O_2 \rightarrow Fe^{3+} + HO^{\bullet} + OH^- \qquad k = 63\text{-}76\ M^{-1}\ s^{-1} \quad \text{(Eq.22)}$$

402 $$Fe^{2+} + S_2O_8^{2-} \rightarrow Fe^{3+} + SO_4^{\bullet-} + SO_4^{2-} \qquad k = 3.0 \times 10^4\ M^{-1}\ s^{-1} \quad \text{(Eq.23)}$$

403 In order to confirm the increased Fe participation under solar light due to ferrate, we substituted Fe(VI)
404 by Fe(III) and the corresponding inactivation was significantly slower (Fig. 3a). Hence, an active
405 participation of Fe(VI) in the process is proposed, and not only as a source of iron. Besides, the
406 Fe(VI)/ Fe(V), Fe(III) and Fe(II) concentrations were followed during the experiments (Figure 4). As
407 can be observed in Figure 4b and 4c, in figure 4b and c, Fe(II) and Fe(III) appear since the commercial
408 potassium ferrate contains a fraction of these two ions. Additionally, the generated amount of Fe (III)
409 is higher due to the fact that Fe(VI) is unstable, and it could be partially oxidized in water to Fe(III),
410 even in few minutes. Regarding the second question, the total iron corresponds to the sum of Fe(II)
411 and Fe(III). It is not stable due to the oxidation of Fe(VI) during the experiment that generates Fe(III)

and is not measured by the Ferrozine method, so the concentration of Fe(III) increases. From the photoreduction of Fe (III), Fe(II)is generated , so the concentration of Fe(III) decreases but Fe(II) increases. Additionally, at pH higher than 3, the iron is not soluble, and they could precipitate as iron hydroxides, which implies the reduction of concentration of total iron (Fe(II) and Fe(III)). Hence, there are many factors that simultaneously affect the iron speciation and in extension, the catalytic disinfection events taking place. .

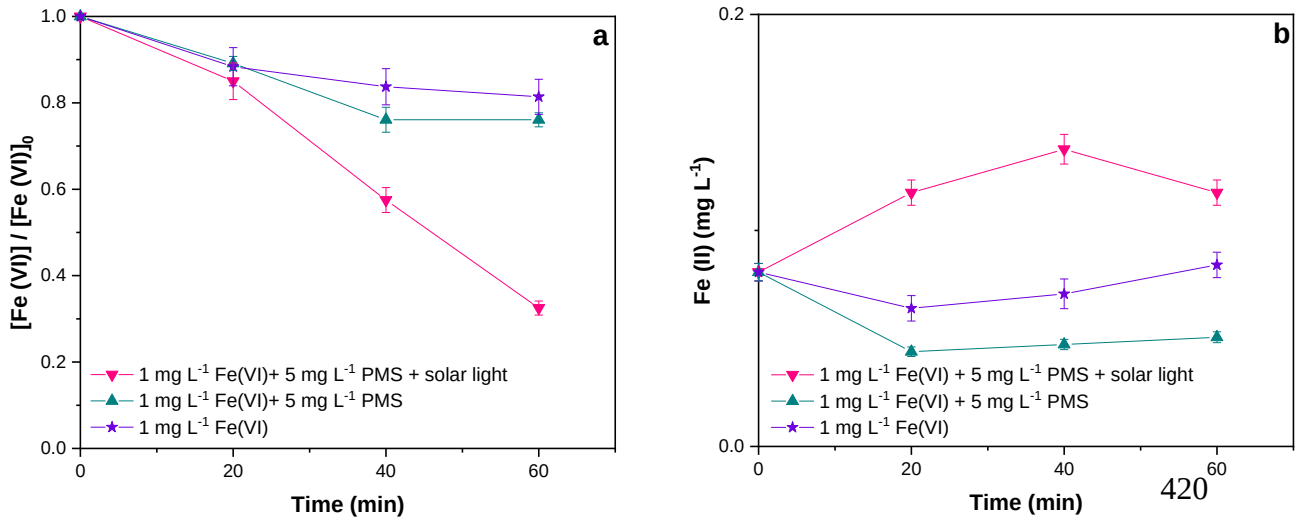

420

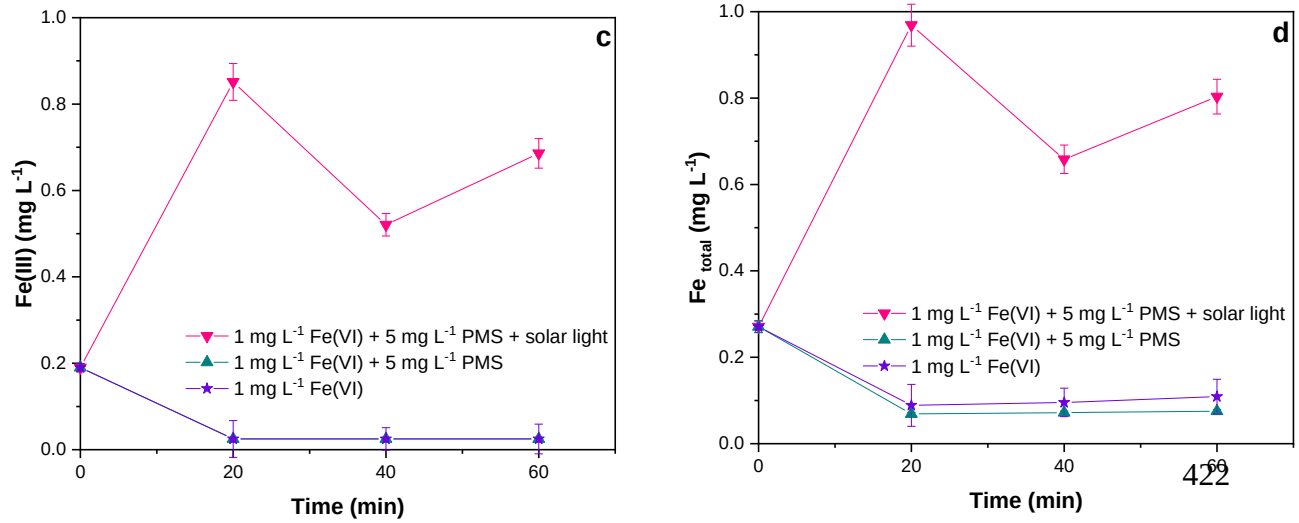

422

Figure 4. a) Ferrate (VI), b) Fe (II), c) Fe (III) and d) Fe total (Fe(II) +Fe(III)) evolution during different experiments [Fe(VI)]= 1 mg L^{-1}; [PMS]= 5 mg L^{-1} and irradiation at 550 W m^{-2}; T= 35 ºC; pH= 6.5.

The concentration of ferrates was reduced by 67.5% in 1 h, while for instance in the Fe(VI)/PMS process less than 20% was consumed. Additionally, the generation of Fe(III) was higher than that in the other experiments: 0.85 mg L^{-1} at 20 min while only 0.02 mg L^{-1} was observed in Fe(VI)/PMS process at the same reaction time. The concentration of Fe(II) was also higher when using Fe(VI)/PMS/solar light compared to the rest of experiments (about x3 times higher). The higher Fe generation was postulated to produce more radicals by reaction with PMS, hence the PMS concentration was followed (see Supplementary Material Fig. S4). PMS reduction was also the highest among all conducted experiments (about 24 %), indicating its higher utilization in the triple-factor process. These tests confirmed the enhancement of the process in bacterial inactivation.

Bearing in mind the different classes of recalcitrant pollutants potentially present in water, in addition to pathogens, the three-factor process was also tested in the removal of 100 μg L^{-1} of SMX under the optimized conditions specified in the caption of Fig. 3b. The results are depicted in Fig. 3b. Similar to *E. coli* inactivation, a synergistic effect was also observed in the removal of this contaminant of concern. Only 8% of SMX degradation was achieved by either photolysis, use of 1 mg L^{-1} of Fe(VI) in dark conditions, addition of 5 mg L^{-1} of PMS also in dark conditions and by the Fe(VI)/solar light process at 1 h. Almost 20% of SMX removal was achieved when mixing PMS with light exposure. However, when PMS, Fe(VI) and light were tested together, more than 70% of SMX degradation was achieved at 1 h. In that case, the calculated factor was $S_{Fe(VI)/PMS/solar}$= 4.18 (Supplementary material Table S2 for see the observed kinetics). The synergistic effect was higher than that observed for bacterial reduction, since SMX is unaffected by germicidal baseline process, such as solar light. These results demonstrated that *E. coli* reduction was achieved more easily than micropollutant removal under the tested conditions. This fact is in agreement with SODIS process which can inactivate bacteria

but had low effect on SMX removal without any improvement as found in the study of Marjanovic and coworkers [7], and Rodriguez-Chueca et al. [3]. These results also hold important implications for water treatment; the combined process merits further investigation and potentially its application for MPs removal.

3.4. Assessment of the involved parameters in the Fe(VI)/ PMS/solar disinfection process

3.4.1. The effect of pH on the efficiency of the combined process

Upon attaining to the efficient combined of Fe(VI)/PMS/solar light process, the effect of initial pH was investigated on the performance of the process on the inactivation of *E. coli*, and the results are shown in Fig. 5. As is observed in Fig. 5, total bacterial inactivation was achieved at 10, 40 and 60 min for the initial pH values of 5.5, 6.5 and 8.5, respectively, while only about 4 log-inactivation was observed when the process was run at the solution pH of 7.5 and at 60 min.

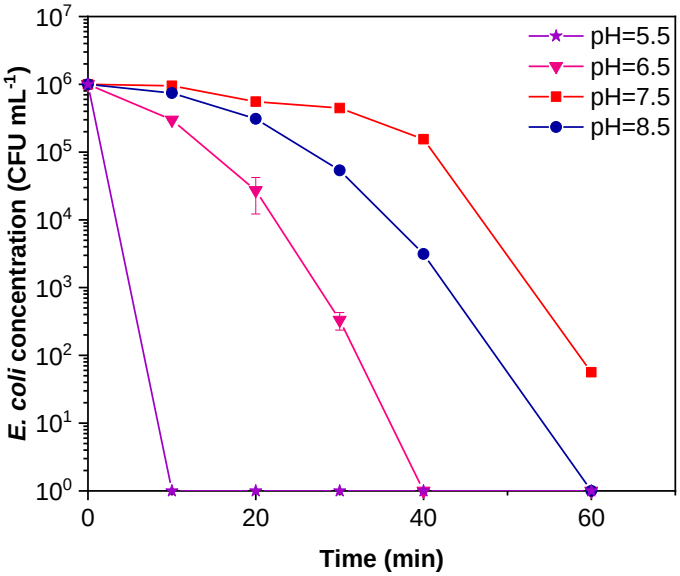

Figure 5. Effect of pH in E. coli inactivation in the combined Fe(VI)/PMS/solar light process. [Fe(VI)] = 1 mg L^{-1}; [PMS] = 5 mg L^{-1} and solar irradiance: 550 W m^{-2}; T= 35 ºC.

471 The differences observed in Figure 5 are related to iron precipitation. At acidic pH, the Fe(III)
472 generated by the reduction of Fe(VI) (Eq.1 and Eq.2) can remain longer in solution and then react with
473 PMS, leading the generation of $HO^{\bullet}$ and achieving relatively fast inactivation rates. Accordingly, at
474 pH 5.5 (that is, the most acidic pH condition among those tested in this work), the required time to
475 inactivate total *E. coli* was the lowest observed and reduced by 30 min the contact time required at pH
476 6.5. At pH 7.5, on its part, above mentioned Fe(III) could be transformed to iron hydroxides more
477 rapidly than at low values of pH [63]. These species have a low solubility in aqueous media, and they
478 precipitate reducing the efficiency of the process. Finally, and although pH 8.5 obviously represent
479 more alkaline media, the slight improvement observed in the inactivation rate compared to pH 7.5
480 conditions can be rationalized by a similar iron precipitation rate in any case compensated by a larger
481 stability of Fe(VI) species under these conditions, as previously reported [28]. Thus, ferrate oxidation
482 would be in that case the main contributor to *E. coli* inactivation.
483
484 *3.4.2. Effect of spectral distribution (emitted wavelength)*
485 Three types of radiation (UVB, UVA and simulated solar irradiation) were explored in the combined
486 Fe(VI), PMS and solar radiation process applied to *E. coli* inactivation. The rationale lies in the wide
487 emission of the Xe lamp of the solar simulator; the emitted light comprises of UVB, UVA and visible
488 wavelengths. By measuring the emitted irradiance values of UVB and UVA, and applying them
489 separately by setting the specific light conditions at the measured ones from the solar light, the
490 contribution of each part of the spectrum can be assessed. Hence, the experimental runs were
491 conducted using artificial radiation in all cases with the same PMS and Fe(VI) concentrations than
492 those applied in the previous experiments. The inactivation potential of this approach is depicted in
493 Figure 6.

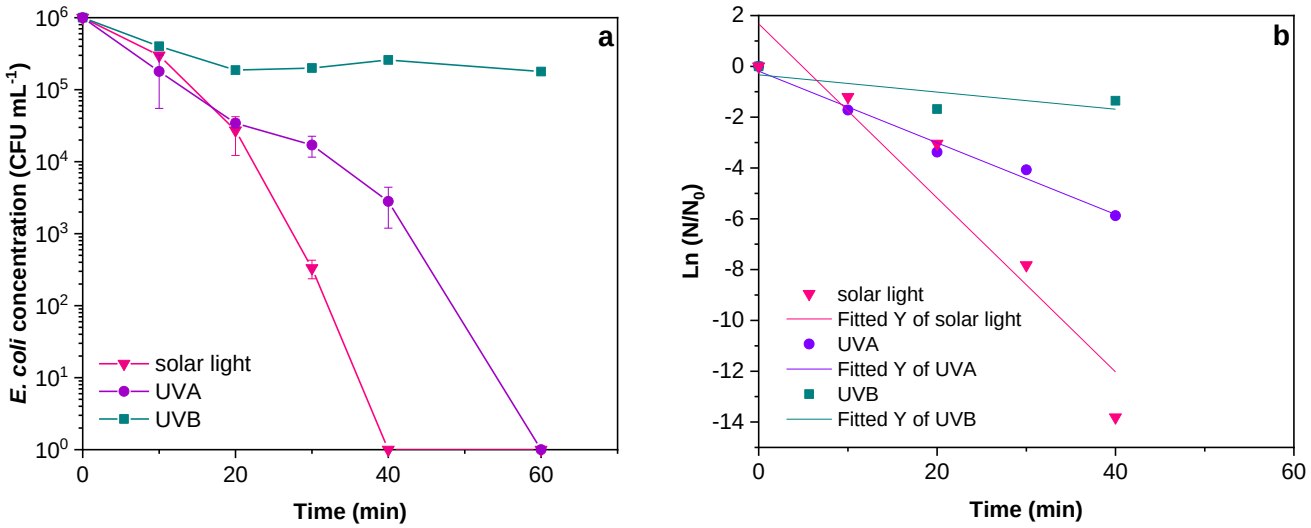

Figure 6. a) Effect of irradiation type in E. coli inactivation in the Fe(VI), PMS and irradiation process using the whole solar spectrum, or the corresponding emitted UVA and UVB irradiation components; b) fittings of pseudo-first order kinetic from the inactivation curves of solar light, UVA and UVB. [Fe(VI)]= 1 mg L^{-1}; [PMS]= 5 mg L^{-1}, solar irradiance: 550 W m^{-2}, containing 20.8 W m^{-2} UVA and 2.8 W m^{-2} UVB, set in the fluorescent tubes system; T= 35 ºC; pH= 6.5.

According to the results displayed in Figure 6, it was found that only 40 min were necessary to achieve the total inactivation of *E. coli* using solar irradiation. However, although in the first 20 min the inactivation using that radiation was very close to UVA light; ultimately, 60 min were required with UVA to reach total inactivation.

According to Giannakis et al., [64] the action mode of solar light against bacteria is an internal photo-Fenton produced in-situ. For its part, UVB irradiation had no significant inhibition effect after 60 min of treatment. Only about 0.5 log-reduction was observed. This fact indicates that the generation of $SO_4^{\bullet-}$ and $HO^{\bullet}$ under these conditions was negligible. The mode of action of UVB radiation against bacteria is direct attack in the double stranded DNA of cell (including pyrimidine dimerization). Moreover, the low bacterial inactivation could come from the formation of $SO_4^{\bullet-}$ and $HO^{\bullet}$ by the breakage of the O-O bond in PMS that requires high energy wavelengths [3]. However, the results

514 suggested that a higher UVB irradiance and resulting dose would be necessary to show a significant
515 *E. coli* inactivation.
516 For its part, UVA light mainly initiates oxidative damage chain reactions involving electron oxidation
517 or singlet oxygen-mediated processes [40]. Additionally, enzymes like catalase, which regulates the
518 concentration of H_2O_2 and Fe-containing structures, are directly affected [3]. This fact causes the
519 accumulation of that reagents inside the bacteria and therefore, the generation of Fenton reactions,
520 resulting in a high $HO^{\bullet}$ formation and cell structure damage [64]. Solar radiation is composed of both
521 UVA and UVB light (plus visible light). Thus, the effects before described occur together, enhancing
522 the overall process efficiency. Observing at 30 min we have almost 1 log with UVB, 2 log with UVA,
523 but 4 log with solar light, or at 40 min almost 1 log with UVB, 2.5 with UVA and 6 with solar light.
524 This means that the different parts are not additive, and/or visible light exerts an influence in the
525 inactivation process by Fe(VI)/PMS. The effect of visible light is rather mild, but it could activate the
526 PMS-Fe complexes enhancing the *E. coli* inactivation. Therefore, judging by the differences of the
527 isolated wavelengths vs. the composite one (i.e., solar light), a possible involvement of visible light in
528 the higher radical's production when solar light was used can be suggested.
529

530 ***3.5. Combined process disinfection effect on different microorganisms***

531 In order to further validate our experiments and the high efficacy of the developed Fe(VI)/PMS/solar
532 light process in the disinfection, the inactivation of various microorganisms was examined in the
533 combined process under optimum experimental conditions (1 mg L^{-1} of Fe(VI) + 5 mg L^{-1} of PMS).
534 The selected microorganism were a wild *E. coli* isolate from secondary wastewater, another gram-
535 Negative bacterium, the *R. planticola* (previously known as *Klebsiella trevisanii*), *B. subtilis* in their
536 vegetative state (before sporulation), a gram-Positive strain isolated from secondary wastewater, the
537 *Enterococcus sp.*, and a eucariotic model yeast, *S. cerevisiae*. The summary of the findings is presented
538 in Fig. 7.

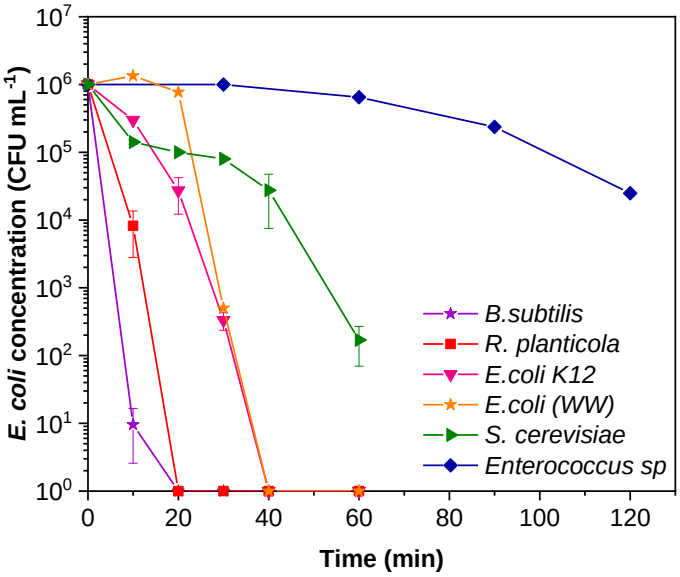

Figure 7. Disinfection of various microorganisms (gram-Negative and gram-Positive bacteria, yeast) under the Fe(VI)/PMS/solar light process; [Fe(VI)]= 1 mg L^{-1}; [PMS]= 5 mg L^{-1}, solar irradiance: 550 W m^{-2}, T= 35 ºC; pH= 6.5.

Compared to the type collection *E. coli* K12 used for the previous tests, the wild isolate presented differences in its inactivation mode, where a prolonged lag period was found. However, the necessary time to reach its total inactivation was identical, suggesting its possibility to survive in harsher environments [65]. *B. subtilis and R. planticola* were inactivated 3.4 and 1.4 times faster, respectively (kinetics can be found in Supplementary information Table S3). Sharing common traits in the structure of their cells, the faster inactivation of *R. planticola* must be attributed to the potential differences in the baseline solar and or PMS disinfection events. *B. subtilis* on the other hand showed profound sensitivity when tested in its vegetative state, a behavior that differs significantly than any tests performed in its spore form [66, 67]. Hence, under the prism of water treatment efficacy in a potential application, the spore form may be of higher concern, judging by the sensitivity of the vegetative cells.

564 *S. cerevisiae* was used as a model microorganism that, although genetically different, its structure
565 resembles the one of the gram-Negative bacteria, albeit with significantly more layers in its cell wall
566 and strong antioxidant responses [68, 69]. After an initial die-off of the sensitive cells, the need to
567 accumulate damages and/or the anti-oxidant events lead to a prolonged lag-phase before killing.
568 However, these types of events were more profound when *Enterococcus sp*. was assayed; insignificant
569 inactivation was observed during the first 60 min. *Enterococcus sp*., as a gram-Positive strain has a
570 different, thicker cell wall structure than *E. coli*, that does not permit its viability get affected easily by
571 extracellular oxidative events, as seen in other works [29, 32]. Besides, the reaction rate of sulfate and
572 hydroxyl radicals when *E. coli* and *Enterococcus sp*. are compared, may explain adequately the low
573 disinfection rate [70, 71] this insinuates a dominant $HO^{\bullet}$ degradation mechanism, plus the gram-
574 Positive components of the outer membrane enhance resistance to bulk oxidation.
575 We should state here that the overall, net synergistic action of the process on each microorganism is
576 not revealing of its isolated components, but gives a good indication of the expected times for
577 inactivation of the various species. Specifically, biological and kinetic factors also have a role; *S.*
578 *cerevisiae* is expected to be more resistant to light alone-induced intracellular oxidative stress [72]
579 than *E. coli*, based on the number of ROS-controlling enzymes, and *E. coli* has a significantly lower
580 second order reaction rate than *E. faecalis* against sulfate radicals [70, 71]. Contextualizing these facts
581 and our results in water treatment, we show that a battery of microbiological tests is necessary to assess
582 the disinfection potential of a process, and that more model strains are required to estimate the times
583 necessary to reach safe levels of microorganisms' presence. Additionally, the performance of the
584 Fe(VI), PMS and solar light combined process in the inactivation of different microorganisms should
585 be investigated in different types of aqueous matrices, such as surface water or wastewater, to
586 understand the potential influence of different compounds contained, such as carbonates, phosphates,
587 and organic matter between others [25, 73, 74].
588

3.6. Integrated proposition for the bacterial inactivation mechanism

3.6.1. Comparison of oxidants

The efficiency of the PDS and H_2O_2-mediated treatment was also assessed on the inactivation of *E. coli* and compared with the PMS-based process. The same molar concentration was used in all cases (0.016 mM, which corresponds to 5 mg L^{-1} of PMS), which may hint towards whether the triple factor disinfection process is leaning towards a sulfate or a hydroxyl-radical dominated process. The results are depicted in Figure 8.

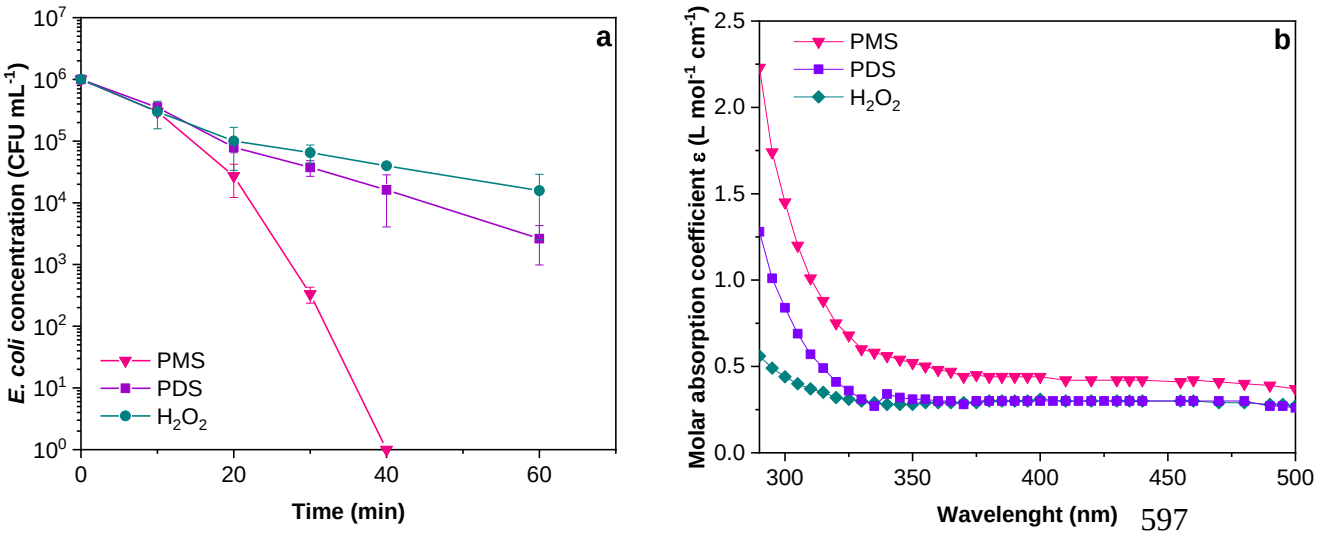

Figure 8. a) Effect of oxidants in E. coli reduction using PMS, PDS or H_2O_2, combined with Fe(VI) and solar light. Conditions: [Fe(VI)]= 1 mg L^{-1}; [PMS; H_2O_2; PDS]= 0.016 mM (on the basis of HSO_5^-) and solar irradiance: 550 W m^{-2}; T= 35 ºC; pH= 6.5; b) molar absorption coefficient for different oxidants.

Considerable differences in the inactivation outcomes were observed between the different oxidants tested. In the presence of PMS, the bacterial inactivation reached the highest efficiency (total inactivation in 40 min). On its part, the process using H_2O_2 or PDS revealed relatively close results: about 2 and 2.5 log-removal, respectively at the end of the treatment. These observations could be explained by the photocleavage of PMS (Eq. 12), which produces $SO_4^{\bullet-}$ and $HO^{\bullet}$, while the analogous

reaction for PDS only generates $SO_4^{\bullet-}$ (Eq.24). For its part, H_2O_2 also produces $HO^\bullet$ (Eq.25). However, the molar absorption coefficient of PMS is higher than both (Figure 8B), hence its photolysis could be leading to higher amounts of radicals. This could be a crucial point; as explained in section 3.3, the generation of $HO^\bullet$ in front of $SO_4^{\bullet-}$ is a key fact to consider, since $HO^\bullet$ in general presents about x10 times higher reactivity with biomolecules than $SO_4^{\bullet-}$ [3, 62, 75].

$S_2O_8^{2-} \xrightarrow{h\nu} 2\ SO_4^{\bullet-}$ φ= 1.4 mol Einstein^{-1} (λ= 254 nm) (Eq.24)

$H_2O_2 \xrightarrow{h\nu} 2\ HO^\bullet$ φ= 0.8 - 0.96 (308-400 nm) (Eq.25)

On the other hand, PMS reacts adequately with Fe(III) (Eq.3) generating $SO_5^{\bullet-}$. However, the rate constant of H_2O_2 with Fe(III) is very slow (Eq.27; k = 0.001-0.01 M^{-1} s^{-1}) [76], and Fe(III) reaction with PDS results in the generation of sulfate radicals and higher valence iron species [77] the kinetics of these reactions are unknown but safely hypothesized to be slow. Additionally, the reaction rate of PMS with Fe(II) is the highest (Eq.4; k = 3.0 x 10^4 M^{-1} s^{-1}), while the rate constant for the PDS- Fe(II) reaction is 12-27 M^{-1} s^{-1} (Eq. 28). Finally, although the reaction of Fe(II) with H_2O_2 generates $HO^\bullet$, the corresponding reaction rate (Eq.26; k = 63-76 M^{-1} s^{-1}) is also lower than that for PMS.

$HSO_5^- + Fe^{3+} \rightarrow Fe^{2+} + SO_5^{\bullet-} + H^+$ (Eq.3)

$HSO_5^- + Fe^{2+} \rightarrow Fe^{3+} + SO_4^{\bullet-} + OH^-$ k= 3.0 x 10^4 M^{-1}s^{-1} (Eq.4)

$H_2O_2 + Fe^{2+} \rightarrow Fe^{3+} + HO^- + HO^\bullet$ k = 63-76 M^{-1}s^{-1} (Eq.26)

$H_2O_2 + Fe^{3+} \rightarrow Fe^{2+} + HO_2^\bullet + H^+$ k = 0.001-0.01 M^{-1}s^{-1} (Eq.27)

$S_2O_8^{2-} + Fe^{2+} \rightarrow Fe^{3+} + SO_4^{\bullet-} + SO_4^{2-}$ k = 12-27 M^{-1}s^{-1} (Eq.28)

$S_2O_8^{2-} + Fe^{3+} + \frac{1}{2}O_2 \rightarrow SO_4^{\bullet-} + Fe^{2+} + SO_4^{2-} + FeO^{2+}$ (Eq.29)

In summary, the photoreaction of oxidants together with the catalytic cycle of iron may explain the considerable differences observed between PMS and the rest of oxidants (PDS and H_2O_2). The Eqs (3, 4, 26-29) also lead to reactive species generation, which makes attribution of the dominant

mechanism complicated. The process must neither be purely hydroxyl or sulfate radical-driven, and further investigation via scavenger experiments is required.

3.6.2. Scavenger experiments

The efficiency of *E. coli* inactivation in presence of MeOH, tBuOH, N_2 and D_2O was investigated in the Fe(VI)/PMS/solar light process, in order to elucidate the corresponding inactivation mechanisms in presence of a radical scavenger (both $HO^{\bullet}$ and $SO_4^{\bullet-}$), only $HO^{\bullet}$, or special conditions that will elucidate the participation of other reactive oxygen species. Fig. 9 displays the bacterial decay registered during the different tests.

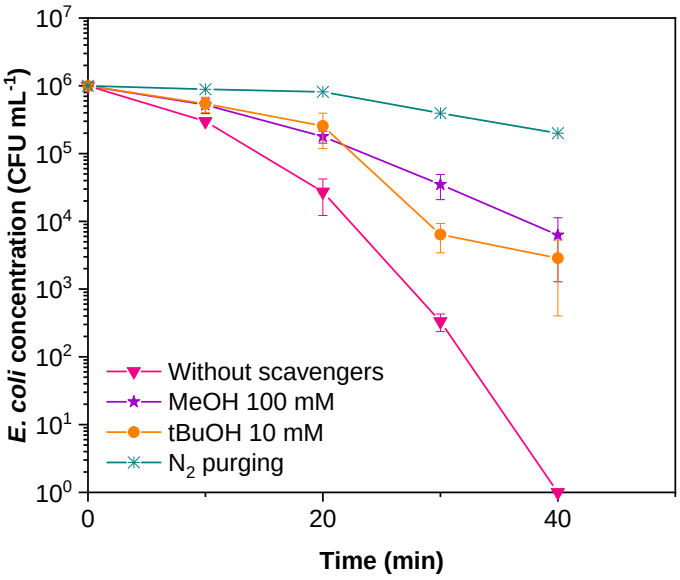

Figure 9. Three-factor inactivation process (Fe(VI), PMS and solar light), radical scavenging experiments and tests performed after N_2 purging. [Fe(VI)]= 1 mg L^{-1}; [PMS]= 5 mg L^{-1} and irradiation at 550 W m^{-2}; [tBuOH]= 10 mM and [MeOH]= 100 mM; ; T= 35 ºC; pH= 6.5.

As explained in section 3.3, it was found that 40 min was necessary to achieve the complete inactivation of *E. coli* in the developed process. The addition of tBuOH and MeOH, however, produced a reduction in the bacterial inactivation rate due to their function of $HO^{\bullet}$, and $HO^{\bullet}$+$SO_4^{\bullet-}$ scavengers,

658 respectively [78]. Two concentrations were tested: 10 and 100 mM of two alcohols in order to ensure
659 the total radical trapping, keeping in mind the sensitivity of bacteria against alcohols (see
660 Supplementary Material Fig. S5).
661 According to the literature, the second order rate constants for reactions of MeOH with hydroxyl and
662 sulfate radicals are, respectively, 9.7 x 10^8 M^{-1} s^{-1} [79] and 1.0 x 10^7 M^{-1} s^{-1} [80]. On its part, tBuOH
663 is an effective scavenger only for hydroxyl radicals with a second order reaction rate of 3.8-7.6 x 10^8
664 M^{-1} s^{-1}, since it reacts much more slowly with sulfate radicals (k= 4.0-9.1 x 10^5 M^{-1} s^{-1}) [81, 82].
665 From the results represented in Fig. S5, it was observed that using two concentrations of tBuOH, the
666 results were very close (about 2.0 x 10^3 CFU mL^{-1} at 40 min), indicating that 10 mM was enough to
667 scavenge $HO^{\bullet}$ in this process. However, when 10 or 100 mM of MeOH were added to the solution 1.6
668 x 10^2 CFU mL^{-1} and 6.3 x 10^3 CFU mL^{-1}, respectively, were observed at 40 min. These results
669 demonstrates that 10 mM of MeOH were not adequate to scavenge all the produced species that
670 inactivate bacteria. On the other hand, in Fig. 9, comparing the results obtained with 100 mM of MeOH
671 and tBuOH it can be observed that the *E. coli* inactivation was quasi-similar in both processes,
672 suggesting that the participation of sulfate radicals was modest. However, the changes in the
673 inactivation rate observed using tBuOH between 20 min and 40 min, suggest an early role for $HO^{\bullet}$, a
674 small but existing for $SO_4^{\bullet-}$, but indicate the action of other inactivation pathways and the presence of
675 different mechanisms of inactivation in the combined process, such as the direct attack of Fe(VI),
676 Fe(IV), PMS, $^1O_2$ and/or solar light.
677 There were however some results that remain elusive. Experiments without O_2 (purging N_2 prior to
678 testing in sealed reactions) disclosed the requirement of oxygen to enable some secondary processes,
679 since a clear reduction of bacterial inactivation was observed at 40 min (residual 2.0 x 10^5 CFU mL^{-1})
680 compared to the test with O_2 (total *E. coli* inactivation). The most plausible scenario is that superoxide,
681 H_2O_2 and or singlet oxygen are participating. Indeed, in Eq.8, the generation of singlet oxygen has
682 been postulated, which is highly germicidal. In order to assess its contribution, the kinetic isotope

683 effect was assessed (see supplementary material Fig. S5), by experimenting in 50% D_2O / 50% H_2O;
684 singlet oxygen is more stable in D_2O than H_2O [83, 84]. The results of the experiments in D_2O, revealed
685 similar (if not slower) bacterial inactivation than in H_2O, moderating the possibility of $^1O_2$
686 participation. Hence other species must participate alongside the $HO^\bullet$ attacks and the direct actions of
687 Fe(VI), PMS and SODIS, such as the peroxymonosulfate and superoxide radicals, ferryl, the generated
688 H_2O_2 and $S_2O_8^{2-}$ from radical recombination, and their activation by iron. The other possibility is that
689 since deuterated H^+ participates with slower kinetics in dismutation and H_2O_2 formation reactions [84],
690 then likely superoxide and hydrogen peroxide may be involved. Our results and hypotheses are in
691 accordance with Xu et al., [85] since from Electron Paramagnetic Resonance (EPR) analyses the
692 involvement of superoxide radical on the oxidation of bisphenol A in the Fe(II)/PMS/UV process was
693 confirmed.

694 *3.6.3. Protein degradation and cell wall oxidation*

695 Having assessed the efficacy of the Fe(VI)/PMS/solar light process, and proposed the main species
696 responsible for the inactivation of bacteria, an assessment of the targets of this oxidative treatment was
697 performed. The total and intracellular protein content of bacteria during treatment was assessed as an
698 indicator of the early and late stage targets of the process, and the malondialdehyde (MDA) formation,
699 as a proxy of cell wall destruction, by lipid peroxidation. The results are summarized in Figure 10.

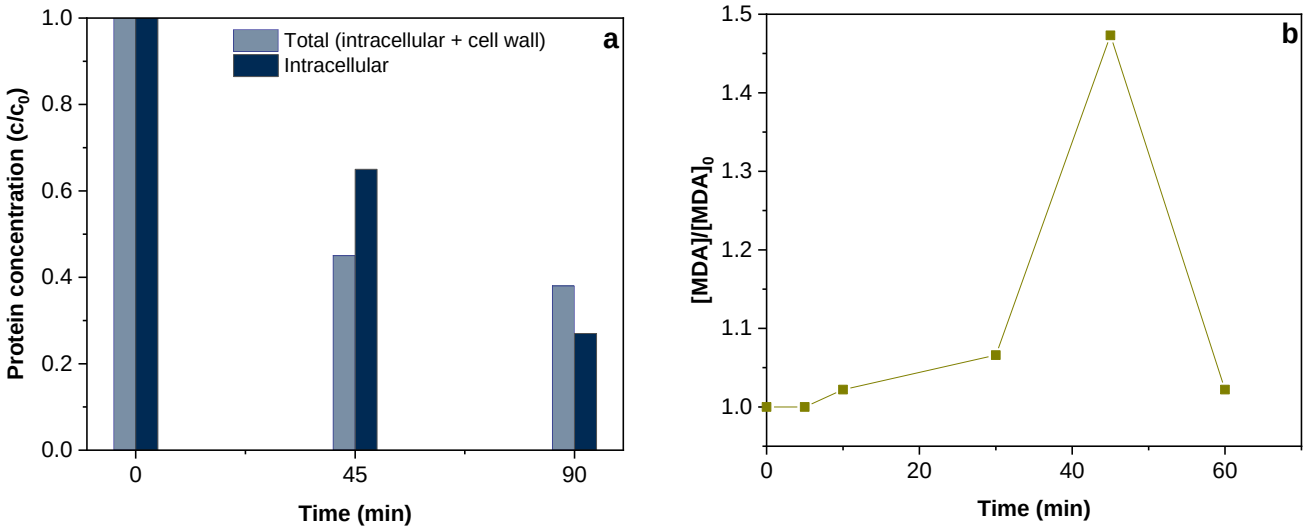

Figure 10. a) Total and Intracellular protein concentration and b) MDA formation during Fe(VI)/ PMS/solar light treatment. Conditions: E. coli concentration: 10^8 CFU mL^{-1}, [PMS]= 25 mg L^{-1}, [Fe(VI)]=5 mg L^{-1} ; T= 35 ºC; pH= 6.5.

In the first stages of the treatment (45 min mark), the total protein content of the cell lysate was reduced by 55% (Fig. 10A). This indicates that the damage was the result of an oxidative process, and not, for instance, influenced heavily from light-induced DNA mutation, as an extreme comparison. From the proteins corresponding to the 55% reduction, only 35% was intracellular proteins, which indicates that the oxidation took place mainly (or initially) in the cell wall rather than the cytoplasm. Prolonging the reaction showed that 62% of the proteins were lost after 90 min of treatment, among which 73% was of intracellular origin. This shows that cell lysis must have occurred, the contents of the cytoplasm were released and were subject to further oxidation by the Fe(VI)/PMS/solar light process. The former suggestion is confirmed by the MDA measurements, which, under the same experimental conditions, revealed the peak of MDA generation at 45 min, i.e., the cell wall oxidation was at its highest rate. The lowering of MDA is logical, since this compound can be degraded during oxidative treatment [56]; at 60 min apparently the oxidation rate of MDA is higher than its production. Consequently, the latter

proposition of cytoplasmic content release is confirmed, due to the disruption of the cell wall indicated by the MDA measurements.

Finally, considering our experimental findings, the prevalent oxidants and action modes, as well as the targets of oxidation, an integrated mechanism of *E. coli* inactivation is given in Figure 11. For simplicity, the actions that have been previously detailed will not be explained or referenced anew.

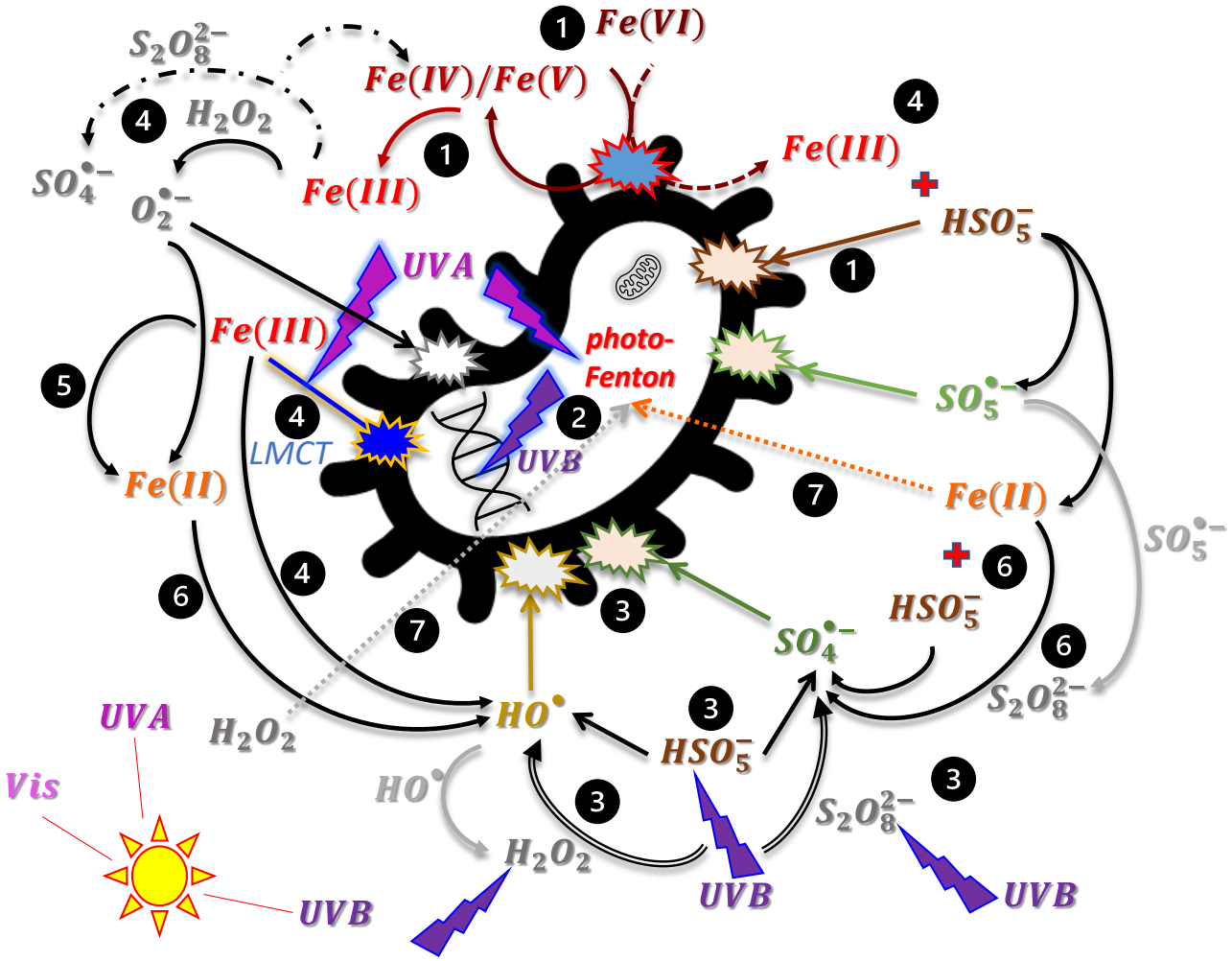

Figure 11. Integrated mechanistic proposition for the inactivation of E. coli under the Fe(VI)/PMS/solar light process. The circled numbers correspond to the pathways explained in the text.

The application of Fe(VI) or PMS alone is an oxidative process, that takes place mostly in the extracellular domain. These compounds can oxidize proteins, lipids, and other components of the cell wall (pathway 1). The by-products of this process are Fe(III) and SO_4^{2-}. Solar light on the other hand,

initiates intracellular photo-catalytic actions, which lead to cell death from the inside, and damages the bacterial genome (pathway 2). The combination of the oxidants with solar light brings an enhancement in the production of radical species in the bulk, mainly $HO^{\bullet}$ and possibly $SO_4^{\bullet -}$, alongside other oxidants' secondary formation, such as H_2O_2 and $S_2O_8^{2-}$, which further fuel radicals' production (pathway 3). The presence of Fe(III) as a by-product is valorized in the reaction with PMS, H_2O_2 and $S_2O_8^{2-}$ and the possible LMCT with the bacterial cell wall, as inactivation forces (pathway 4). More importantly, Fe(III) from Fe(VI) drives the formation of Fe(II) via its photo-reduction or superoxide mediated reduction (pathway 5), which might also contribute to bacterial inactivation. In turn, Fe(II) reaction with the inorganic peroxides formed (pathway 6), the diffusion inside the cell and the subsequent aggravation of intracellular oxidation (pathway 7), all contribute to an accelerated bacterial inactivation. Cells have their wall structure affected as well as proven cytoplasmic damages after their partial or complete lysis.

4. Conclusions

The low performance of Fe(VI) or PMS by themselves or combined with solar light (two-factor disinfection) makes necessary the use of reducing agents to diminish the treatment time to disinfect and/or decontaminate water. In this way, the triple-factor inactivation (Fe(VI)/PMS/solar light) reached 6-log reduction in only 40 minutes, which was faster than Fe(VI) or PMS combined with solar light. In the case of sulfamethoxazole, more than 80% removal was achieved with Fe(VI)/PMS/solar light system, while only about 20% was observed with single and double-factor treatment. Additionally, the Fe(VI)/PMS/solar light process promotes a synergistic disinfection in a wide pH operation, and it gives the possibility to re-valorize the Fe(III) generation that would otherwise precipitate fast at neutral pH.

Light spectrum effects and inorganic peroxide tests, alongside the scavenger tests performed, showed that bacterial inactivation is caused by the joint action of $HO^{\bullet}$ with the direct attack of Fe(VI), PMS and SODIS. Experiments without O_2 exposed the requirement of oxygen to enable further processes, without excluding the possible involvement of superoxide or hydrogen peroxide.

Considering all the above information, the integrated mechanism for the *E.coli* inactivation was proposed. In total, a combined extracellular/intracellular process is achieved. This has important positive outlooks, since multi-level damage may lead to cell death instead of plain inactivation or induction of a viable-but not cultivable-state and makes bacteria less prone to regrowth after repair of their damages. On the other hand, the tests performed with different microorganisms revealed that a battery of microbiological tests is necessary to assess the disinfection potential of the Fe(VI)/PMS/solar light process, as well as any new disinfection process for that matter, and that more model strains are required to estimate the times necessary to reach safe levels of microorganisms' presence.

5. Acknowledgements

Stefanos Giannakis would like to acknowledge the Spanish Ministry of Science, Innovation and Universities (MICIU) for the Ramón y Cajal Fellowship (RYC2018-024033-I) and the 'NAVIA' Project (PID2019-110441RB-C32). Núria López is grateful to the Spanish Ministry of Science and Innovation (aids for mobility for short-term research stays of FPU predoctoral staff, grant Nº FPU-16/02101) which provided the economic support required to carry out the research stay at UPM.

6. References

[1] K. G. McGuigan, R. M. Conroy, H-J. Mosler, M. du Preez, E. Ubomba-Jaswa, P. Fernandez-Ibañez, Solar water disinfection (SODIS): A review from bench-top to roof-top, Journal of Hazardous Materials 235-236 (2012) 29-46.

[2] World Health Organization. 14 June 2019. Drinking-water. https://www.who.int/news-room/fact-sheets/detail/drinking-water

[3] J. Rodríguez-Chueca, S. Giannakis, M. Marjanovic, M. Kohantorabi, M. Reza Gholami, D. Grandjean, L. F. de Alencastro, C. Pulgarín, Solar assisted bacterial disinfection and removal of contaminants of emerging concern by Fe^{2+}-activated HSO_5- vs. $S2O_8^{2-}$ in drinking water, Applied Catalysis B: Environmental 248 (2019) 62-72.

[4] X. Zhang, M. Feng, C. Luo, N. Nesnas, C-H. Huang, V. K. Sharma, Effect of metal ions on oxidation of micropollutants by Fe(VI): Enhancing role of Fe^{IV} species, Environmental Science & Technology 55 (2021) 623-633.

[5] X. Yu, Q. Sui, S. Lyu, W. Zhao, J. Liu, Z. Cai, G. Yu, D. Barceló, Municipal solid waste landfills: An underestimated source of PPCPs in the water environment, Environmental Science & Technology 54 (2020) 9757-9768.

[6] U. Nations, Resolut. Adopt. by Gen. Assem. UN Doc. A/, (2015).

[7] A. Meireles, E. Giaouris, M. Simoes, Alternative disinfection methods to chlorine for use in the fresh-cut industry, Food Research International, 82 (2016) 71-85.

[8] N. López-Vinent, A. Cruz-Alcalde, J. Giménez, S. Esplugas, Mixtures of chelating agents to enhance photo-Fenton process at natural pH: Influence of wastewater matrix on micropollutant removal and bacterial inactivation, Science of the Total Environmental 786 (2021) 147416.

[9] N. López-Vinent, A. Cruz-Alcalde, J. A. Malvestiti, P. Marco, J. Giménez, S. Esplugas, Organic fertilizer as a chelating agent in photo-Fenton at neutral pH with LEDs for agricultural wastewater reuse: Micropollutant abatement and bacterial inactivation, Chemical Engineering Journal 388 (2020) 124246.

[10] A. M. Gorito, J. F. J. R. Pesqueira, N. F. F. Moreira, A. R. Ribeiro, M. F. R. Pereira, O. C. Nunes, C. M. R. Almeida, A. M. T. Silva, Ozone-based water treatment (O_3, O_3/UV, O_3/H_2O_2) for removal of organic micropollutants, bacteria inactivation and regrowth prevention, Journal of Environmental Chemical Engineering 9 (2021) 105315.

[11] A. Cibati, R. Gonzalez-Olmos, S. Rodriguez-Mozaz, G. Buttiglieri, Unravelling the performance of UV/H_2O_2 on the removal of pharmaceuticals in real industrial, hospital, grey and urban wastewaters, Chemosphere 290 (2022) 133315.

[12] N. López-Vinent, A. Cruz-Alcalde, J. Giménez, S. Esplugas, C. Sans, Improvement of the photo-Fenton process at natural condition of pH using organic fertilizers mixtures: Potential application to agricultural reuse of wastewater, Applied Catalysis B: Environmental 290 (2021) 120066.

[13] J. Li, X. Dou, H. Qin, Y. Sun, D. Yin, X. Guan, Characterization methods of zerovalent iron for water treatment and remediation, Water Research (2019) 70-85.

[14] S. O. Ganiyu, M. Zhou, C. A. Martínez-Huitle, Heterogeneous electro-Fenton and photoelectro-Fenton processes: A critical review of fundamental principles and application for water/wastewater treatment, Applied Catalysis B: Environmental 235 (2018) 103-129.

[15] V. K. Sharma, R. Zboril, R.S. Varma, Ferrates: Greener oxidants with multimodal action in water treatment technologies, Accounts of Chemical Research 48 (2015) 182-191.

[16] H. Liu, X. Pan, J. Chen, Y. Qi, R. Qu, Z. Wang, Kinetics and mechanism of the oxidative degradation of parathion by Ferrate(VI), Chemical Engineering Journal 365 (2019) 142-152.

[17] T. Yang, L. Wang, Y. Liu, J. Jiang, Z. Huang, S-Y. Pang, H. Cheng, D. Gao, J. Ma, Removal of Organoarsenic with Ferrate and Ferrate Resultant Nanoparticles: Oxidation and Adsorption, Environmental Science & Technology 52 (2018) 13325−13335.

[18] T. Yang, L. Wang, Y. Liu, Z. Huang, H. He, X. Wang, J. Jiang, D. Gao, J. Ma, Comparative study on ferrate oxidation of BPS and BPAF: Kinetics, reaction mechanism, and the improvement on their biodegradability, Water Research 148 (2019) 115-125.

[19] L. Hu, M. A. Page, T. Sigstam, T. Kohn, B. J. Mariñas, T. J. Strathmann, Inactivation of Bacteriophage MS2 with Potassium Ferrate(VI), Environmental Science & Technology 46 (2012) 12079−12087.

[20] V.K. Sharma, Disinfection performance of Fe(VI) in water and wastewater: a review, Water Science &Technology 55 (2007) 225–232.

[21] B. Shao, H. Dong, B. Sun, X. Guan, Role of Ferrate (IV) and Ferrate (V) in activating Fe(VI) by calcium sulfite for enhanced oxidation of organic contaminants, Environmental Science & Technology 53 (2019) 894-902.

827 [22] J. Shin, V. Von Gunten, D.A. Reckhow, S. Allard, Y. Lee, Reactions of Fe(VI) with iodine and hypoiodous acid:
828 Kinetics, pathways, and implications for the fate of iodide during water treatment, Environmental Science & Technology
829 52 (2018) 7458-7467.
830 [23] C. Luo, M. Feng, V.K. Sharma, C. H. Huang, Oxidation of pharmaceuticals by Fe(VI) in hydrolyzed urine: Effects of
831 major inorganic constituents, Environmental Science & Technology 53 (2019) 5271-5281.
832 [24] M. Feng, X, Wang, J. Chen, R. Qu, Y.Sui, L. Cizmas, Z. Wang, V. K. Sharma, Degradation of fluoroquinolone
833 antibiotics by Fe(VI) : Effects of water constituents and oxidized products, Water Research 103 (2016) 48-57.
834 [25] C. Li, H. Lin, A. Armutlulu, R. Xie, Y. Zhang, X. Meng, Hydroxylamine-assisted catalytic degradation of
835 ciprofloxacin in ferrate/persulfate system, Chemical Engineering Journal 360 (2019) 612-620.
836 [26] M. Feng, L. Cizmas, Z. Wang, V. K. Sharma, Synergistic effect of aqueous removal of fluorquinolones by a combined
837 use of peroxymonosulfate and Fe(VI), Chemosphere 177 (2017) 144-148.
838 [27] C. He, X. Zhang, P. Lv, H. Sui, X. Li, L. He, Efficient remediation of o-dichlorbenzene-contaminated soil using
839 peroxomonosulfte-ferrate-FeS hybrid oxidation system, Journal of the Taiwan Institute of Chemical Engineers 119 (2021)
840 23-32.
841 [28] M. Karbasi, F. Karimzadeh, K. Raeissi, S. Giannakis, C. Pulgarin, Improving visible light photocatalytic inactivation
842 of *E. coli* by inducing highly efficient radical pathways through peroxymonosulfate activation using 3-D, surface-enhanced,
843 reduced graphene oxide (rGO) aerogels, Chemical Engineering Journal 396 (2020) 125189.
844 [29] S. Mohammadi, G. Moussavi, S. Shekoohiyan, M. L. Marín, F. Boscá, S. Giannakis, A continuous-flow catalytic
845 process with natural hematite-alginate beads for effective water decontamination and disinfection: Peroxymonosulfate
846 activation leading to dominant sulfate radical and minor non-radical pathways, Chemical Engineering Journal 411 (2021)
847 127738.
848 [30] M. H. Wu, J. Shi, H. P. Deng, Metal doped manganese oxide octahedral molecular sieve catalysis for degradation of
849 diclofenac in the presence of peroxymonosulfate, Arabian Journal of Chemistry 11 (2018) 924-934.
850 [31] S. Fukuchi, R. Nishimoto, M. Fukushima, Q. Zhu, Effects of reducing agents on the degradation of 2,4,6-
851 tribromophenol in a heterogeneous Fenton-like system with an iron-loaded natural zeolite, Applied Catalysis B:
852 Environmental 147 (2014) 411-419.
853 [32] S. Guerra-Rodríguez, N. Cediel, E. Rodríguez, J. Rodríguez-Chueca, Photocatalytic activation of sulfite using Fe(II)
854 and Fe(III) for *Enterococcus* sp. Inactivation in urban wastewater, Chemical Engineering Journal 408 (2021) 127326.

[33] C. Casado, J. Moreno-SanSegundo, I. De la Obra, B. Esteban García, J. A. Sánchez Pérez, J. Marugán, Mechanistic modelling of wastewater disinfection by the photo-Fenton process at circumneutral pH, Chemical Engineering Journal, 403 (2021) 126335.

[34] M. Minella, S. Giannakis, A. Mazzavillani, V. Maurino, C. Minero, D. Vione, Phototransformation of Acesulfame K in surface waters: Comparison of two techniques for the measurement of the second-order rate constants of indirect photodegradation, and modelling of photoreaction kinetics, Chemosphere 186 (2017) 185-192.

[35] P. Ozores Diez, S. Giannakis, J. Rodríguez-Chueca, D. Wang, B. Quilty, R. Devery, K. McGuigan, C. Pulgarin, Enhancing solar disinfection (SODIS) with the photo-Fenton or the Fe^{2+}/peroxymonosulfate-activation process in large-scale plastic bottles leads to toxicologically safe drinking water, Water Research 186 (2020) 116387.

[36] E. Gentil Mbonimpa, B. Vadheim, E. R. Blatchley III, Continuous-flow solar UVB disinfection reactor for drinking water, Water Research 46 (2012) 2344-2355.

[37] L. Feng, C. Peillex-Delphe, C. Lü, D. Wang, S. Giannakis, C. Pulgarin, Employing bacterial mutations for the elucidation of photo-Fenton disinfection: Focus on the intracellular and extracellular inactivation mechanisms induced by UVA and H_2O_2, Water Research 182 (2020) 116049.

[38] I. de la Obra, B. Esteban García, J. L. García Sánchez, J. L. Casas López, J. A. Sánchez Pérez, Low cost UVA-LED as a radiation source for the photo-Fenton process: a new approach for micropollutant removal from urban wastewater, Photochemical & Photobiological Sciences 16 (2017) 72-78.

[39] N. Hasan, S. Kim, M. S. Kim, N. T. Thao Nguyen, C. Lee, J. Kim, Visible light-induced activation of peroxymonosulfate in the presence of ferric ions for the degradation of organic pollutants, Separation and Purification Technology 240 (2020) 116620.

[40] S. Giannakis, M. I. Polo López, D. Spuhler, J. A. Sánchez Pérez, P. Fernández Ibáñez, C. Pulgarin, Solar disinfection is an augmentable, *in situ*-generated photo-Fenton reaction-Part 1: A review of the mechanisms and the fundamental aspects of the process, Applied Catalysis B: Environmental 199 (2016) 199-223.

[41] R. E. Núñez-Salas, J. Rodríguez-Chueca, A. Hernández-Ramírez, E. Rodríguez, M. L. Maya-Treviño, Evaluation of B-ZnO on photocatalytic inactivation of *Eschericjia coli* and *Enterococcus* sp, Journal of Environmental Chemical Engineering 9 (2021) 104940.

[42] S. Waclawek, K. Grübel, M. Cerník, Simple spectrophotometric determination of monopersulfate, Spectrochimica Acta Part A: Molecular and Biomolecular Spectroscopy 149 (2015) 928-933.

[43] Y-L. Wei, Y-S. Wang, C-H. Liu, Preparation of potassium ferrate from spent steel pickling liquid, Metals 5 (2015) 1770-1787.

[44] E. Viollier, P.W. Inglett, K. Hunter, A.N. Roychoudhury, P. Van Cappellen, The ferrozine method revisited: Fe(II)/Fe(III) determination in natural waters, Applied Geochemistry 15 (2000) 785-790.

[45] N. J. Kruger, The Bradford Method For Protein Quantification BT- The Protein Protocols Handbook, in: J. M. Walker (Ed.), Humans Press, Totowa, NJ (2009) 17-24.

[46] A. Zeb, F. Ullah, A Simple Spectrophotometric Method for the Determination of Thiobarbituric Acid Reactive Substances in Fried Fast Foods, Journal of Analytical Methods in Chemistry, (2016), Article ID 9412767, 5 pages.

[47] I. Berruti, I. Oller, M. I. Polo-López, Direct oxidation of peroxymonosulfate under natural solar radiation: Accelerating the simultaneous removal of organic contaminants and pathogens from water, Chemosphere 279 (2021) 130555.

[48] J. Wang, S. Wang, Activation of persulfate (PS) and peroxymonosulfate (PMS) and application for the degradation emerging contaminants, Chemical Engineering Journal 334 (2018) 1502–1517.

[49] M. Brasca, S. Morandi, R. Lodi, A. Tamburini, Redox potential to discriminate among species of lactic acid bacteria, Journal of Applied Microbiology 103 (2007) 1516–1524.

[50] O.N. Oktyabrskii, G.V. Smirnova, Redox potential changes in bacterial cultures under stress conditions, Microbiology 81 (2012) 131–142.

[51] D. Spuhler, A.J. Rengifo-Herrera, C. Pulgarin, The effect of Fe^{2+}, Fe^{3+}, H_2O_2 and the photo-Fenton reagent at near neutral pH on the solar disinfection (SODIS) at low temperatures of water containing Escherichia coli K12, Applied Catalysis B: Environmental 96 (2010)126–141.

[52] M. Marjanovic, S. Giannakis, D. Grandjean, L. F. de Alencastro, C. Pulgarin, Effect of μM Fe addition, mild heat and solar UV on sulfate radical-mediated inactivation of bacteria, viruses, and micropollutant degradation in water, Water Research 140 (2018) 220-231.

[53] M. Kohantorabi, G. Moussavi, S. Giannakis, A review of the innovations in metal- and carbon-based catalysts explored for heterogeneous peroxymonosulfate (PMS) activation, with focus on radical vs. non-radical degradation pathways of organic contaminants, Chemical Engineering Journal 411 (2021) 127957.

[54] D. Ouyang, Y. Chen, J. Yan, L. Qian, L. Han, M. Chen, Activation mechanism of peroxymonosulfate by biochar for catalytic degradation of 1,4-dioxane: Important role of biochar defect structures, Chemical Engineering Journal 370 (2019) 614-624.

[55] L. Clarizia, D. Russo, I. Di Somma, R. Marotta, R. Andreozzi, Homogeneous photo-Fenton processes at near neutral pH: A review, Applied Catalysis B: Environmental 209 (2017) 358-371.

[56] C. Ruales-Lonfat, N. Benítez, A. Sienkiewicz, C. Pulgarín, Deleterious effect of homogeneous and heterogeneous near-neutral photo-Fenton system on *Escherichia coli*. Comparison with photo-catalytic action of TiO_2 during cell envelope disruption, Applied Catalysis B: Environmental 160-161 (2014) 286-297.

[57] I. García-Fernández, M. Polo-López, I. Oller, P. Fernández-Ibáñez, Bacteria and fungi inactivation using Fe^{3+}/sunlight, H_2O_2/sunlight and near neutral photo-Fenton: a comparative study, Applied Catalysis B: Environmental 121–122 (2012) 20–29.

[58] S. Wu, H. Li, X. Li, H. He, C. Yang, Performances and mechanisms of efficient degradation of atrazine using peroxymonosulfate and ferrate as oxidants, Chemical Engineering Journal 353 (2018) 533-541.

[59] Y-H. Guan, J. Ma, X-C Li, J-Y Fang, L-W Chen, Influence of pH on the Formation of Sulfate and Hydroxyl Radicals in the UV/Peroxymonosulfate System, Environmental Science & Technology 45 (2011) 9308–9314.

[60] Q. Yang, Y. Ma, F. Chen, F. Yao, J. Sun, S. Wang, K. Yi, L. Hou, X. Li, D. Wang, Recent advances in photo-activated sulfate radical-advanced oxidation process (SR-AOP) for refractory organic pollutants removal in water, Chemical Engineering Journal 378 (2019) 122149.

[61] Y. Qi, J. Wei, Ruijuan Qu, G. Al-Basher, X. Pan, A. A. Dar, A. Shad, D. Zhou, Z. Wang, Mixed oxidation of aqueous nonylphenol and triclosan by thermally activated persulfate: Reaction kinetics and formation of co-oligomerization products, Chemical Engineering Journal 403 (2021) 126396.

[62] G.P. Anipsitakis, T.P. Tufano, D.D. Dionysiou, Chemical and microbial decontamination of pool water using activated potassium peroxymonosulfate, Water Research 42 (2008) 2899–2910.

[63] B. Morgan, O. Lahav, The effect of pH on the kinetics of spontaneous Fe(II) oxidation by O_2 in aqueous solution--basic principles and a simple heuristic description, Chemosphere 68 (2007) 2080-2084.

[64] S. Giannakis, Analogies and differences among bacterial and viral disinfection by the photo-Fenton process at neutral pH: a mini review, Environmental Science and Pollution Research 25 (2018) 27676-27692.

[65] J. D. van Elsas, A. V. Semenov, R. Costa, J. T. Trevors, Survival of *Escherichia coli* in the environment: fundamental and public health aspects, The ISME Journal 5 (2011) 173-183.

[66] P. Sun, C. Tyree, C-H. Huang, Inactivation of Escherichia coli, Bacteriophage MS2, and Bacillus Spores under UV/H_2O_2 and UV/Peroxydisulfate Advanced Disinfection Conditions, Environmental Science & Technology 50 (2016) 4448-4458.

[67] F. Zeng, S. Cao, W. Jin, X. Zhou, W. Ding, R. Tu, S-F. Han, C. Wang, Q. Jiang, H. Huang, F. Ding, Inactivation of chlorine-resistant bacterial spores in drinking water using UV irradiation, UV/Hydrogen peroxide and UV/Peroxymonosulfate: Efficiency and mechanism, Journal of Cleaner Production 243 (2020) 118666.

[68] M. D. Temple, G. G. Perrone, I. W. Dawes, Complex cellular responses to reactive oxygen species, Trends in cell biology 15 (2005) 319-326.

[69] S. Giannakis, C. Ruales-Lonfat, S. Thabet, P. Cotton, C. Pulgarin, Castles fall from inside: Evidence for dominant internal photo-catalytic mechanisms during treatment of *Saccharomyces cerevisiae* by photo-Fenton at near-neutral pH, Applied Catalysis B: Environmental 185 (2016) 150-162.

[70] R. Xiao, K. Liu, L. Bai, D. Minakata, Y. Seo, R.K. Goktas, et al, Inactivation of pathogenic microorganisms by sulfate radical: present and future, Chemical Engineering Journal 371 (2019) 222-232

[71] R. Xiao, L. Bai, K. Liu, Y. Shi, D. Minakata, C.H. Huang, et al, Elucidating sulfate radical-mediated disinfection profiles and mechanisms of *Escherichia coli* and *Enterococcus faecalis* in municipal wastewater, Water Research 173 (2020) 115552.

[72] S. Giannakis, C. Ruales-Lonfat, S. Rtimi, S. Thabet, P. Cotton, C. Pulgarin, Castles fall from inside: Evidence for dominant internal photo-catalytic mechanisms during treatment of Saccharomyces cerevisiae by photo-Fenton at near-neutral pH, Applied Catalysis B: Environmental 185 (2016) 150-162.

[73] Z-S Huang, L. Wang, Y-L. Liu, J. Jiang, M. Xue, C-B. Xu, Y-F. Zhen, Y-.C Wang, J. Ma, Impact of Phosphate on Ferrate Oxidation of Organic Compounds: An Underestimated Oxidant, Environmental Science & Technology 52 (2018) 13897−13907.

[74] X. Wang, Y. Liu, Z. Huang, L. Wang, Y. Wang, Y. Li, J. Li, J. Qi, J. Ma, Rapid oxidation of iodide and hypoiodous acid with ferrate and no formation of iodoform and monoiodoacetic acid in the ferrate/I−/HA system, Water Research 144 (2018) 592-602.

[75] S. Goldstein, D. Aschengrau, Y. Diamant, J. Rabani, Photolysis of Aqueous H_2O_2: Quantum Yield and Applications for Polychromatic UV Actinometry in Photoreactors, Environ. Sci. Technol. 41 (2007) 7486–7490.

[76] C. Walling and A. Goosen, Mechanism of the ferric ion catalyzed decomposition of hydrogen peroxide. Effect of organic substrates, Journal of American Chemical Society 95 (1973) 2987–2991.

[77] S. Giannakis, K-Y. A. Lin, F. Ghanbari, A review of the recent advances on the treatment of industrial wastewaters by Sulfate Radical-based Advanced Oxidation Processes (SR-AOPs), Chemical Engineering Journal 406 (2021) 127083.

[78] A. Cruz-Alcalde, N. López-Vinent, R. S. Ribeiro, J. Giménez, C. Sans, A. M. T. Silva, Persulfate activation by reduced graphene oxide membranes: Practical and mechanistic insights concerning organic pollutants abatement, Chemical Engineering Journal 427 (2022) 130994.

[79] G. V. Buxton, C. L. Greenstock, W. P. Helman, A. B. Ross, Critical Review of rate constants for reactions of hydrated electrons, hydrogen atoms and hydroxyl radicals (•OH/•O^-) in aqueous solution, Journal of Physical and Chemical Reference Data 17 (1988) 513-886.

[80] C. L. Clifton and R. E. Huie, Rate constants for hydrogen abstraction reactions of the sulfate radical, SO4-. Alcohols, International Journal of Chemical Kinetics 21 (1989) 677-687.

[81] E. Hayon, A. Treinin, J. Wilf, Electronic spectra, photochemistry, and autoxidation mechanism of the sulfite-bisulfite-pyrosulfite systems. SO2-, SO3-, SO4-, and SO5- radicals, Journal of American Chemical Society 94 (1972) 47–57.

[82] G. Wu, Y. Katsumura, G. Chu, Photolytic and radiolytic studies of $SO_4^{\bullet-}$ in neat organic solvents, Physical Chemistry Chemical Physics 2 (2000) 5602–5605.

[83] E. A. Serra-Galvis, J. A. Troyon, S. Giannakis, R. A. Torres-Palma, C. Minero, D. Vione, C. Pulgarin, Photoinduced disinfection in sunlit natural waters: Measurement of the second order inactivation rate constants between *E. coli* and photogenerated transient species, Water Research 147 (2018) 242-253.

[84] M. Kohantorabi, S. Giannakis, M. Reza Gholami, L. Feng, C. Pulgarin, A systematic investigation on the bactericidal transient species generated by photo-sensitization of natural organic matter (NOM) during solar and photo-Fenton disinfection of surface waters, Applied Catalysis B: Environmental 244 (2019) 983-995.

[85] L. Xu, L. Qi, Y. Han, W. Lu, J. Han, W. Qiao, X. Mei, Y. Pan, K. Song, C. Ling, L. Gan, Improvement of Fe^{2+}/peroxymonosulfate oxidation of organic pollutants by promoting Fe^{2+} regeneration with visible light driven g-C3N4 photocatalysis, Chemical Engineering Journal 430 (2022) 132828.

Supplementary Information for

Improving ferrate disinfection and decontamination performance at neutral pH by activating peroxymonosulfate under solar light

Núria López-Vinent [abc1]*, ***Alberto Cruz-Alcalde*** [ab1], ***Gholamreza Moussavi*** [d], ***Isabel del Castillo Gonzalez*** [b], ***Aurelio Hernandez Lehmann*** [b], ***Jaime Giménez*** [a], ***Stefanos Giannakis*** [b**]

[a]*Department of Chemical Engineering and Analytical Chemistry, Faculty of Chemistry, University of Barcelona, C/Martí i Franqués 1, 08028 Barcelona, Spain.*

[b]*Universidad Politécnica de Madrid, E.T.S. de Ingenieros de Caminos, Canales y Puertos, Departamento de Ingeniería Civil: Hidráulica, Energía y Medio Ambiente, Unidad docente Ingeniería Sanitaria, C/Profesor Aranguren s/n, 28040 Madrid, Spain.*

[c]*Department of Environmental Chemistry, IDAEA-CSIC, C/ Jordi Girona 18, 08034 Barcelona, Spain*

[d]*Department of Environmental Health Engineering, Faculty of Medical Sciences, Tarbiat Modares University, Tehran, Iran*

***Corresponding author**: Núria López-Vinent (nuria.lopez@ub.edu)

****Corresponding author**: Stefanos Giannakis (Stefanos.Giannakis@upm.es)

[1] NLV and ACA have contributed equally to this work.

Table of contents

Figure S1. Suntest solar simulator light wavelength emission spectrum for Xe lamps (Manufacturer: Suntest Xenon Test-Instruments Brochure)

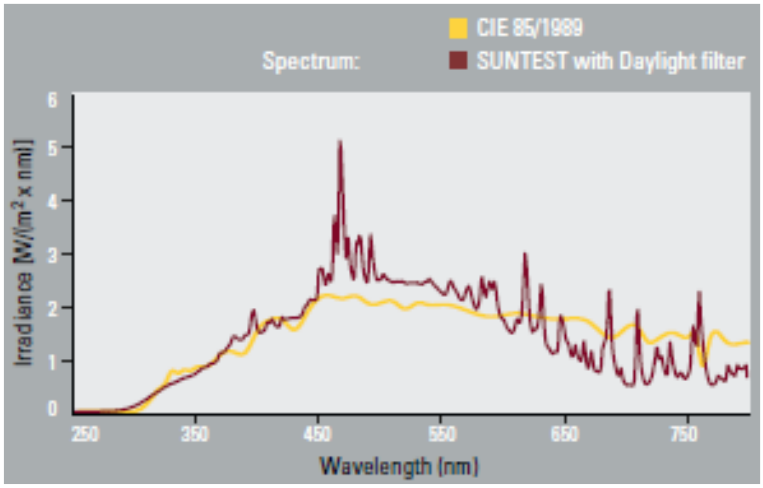

Figure S2. Light spectra for UVB lamps

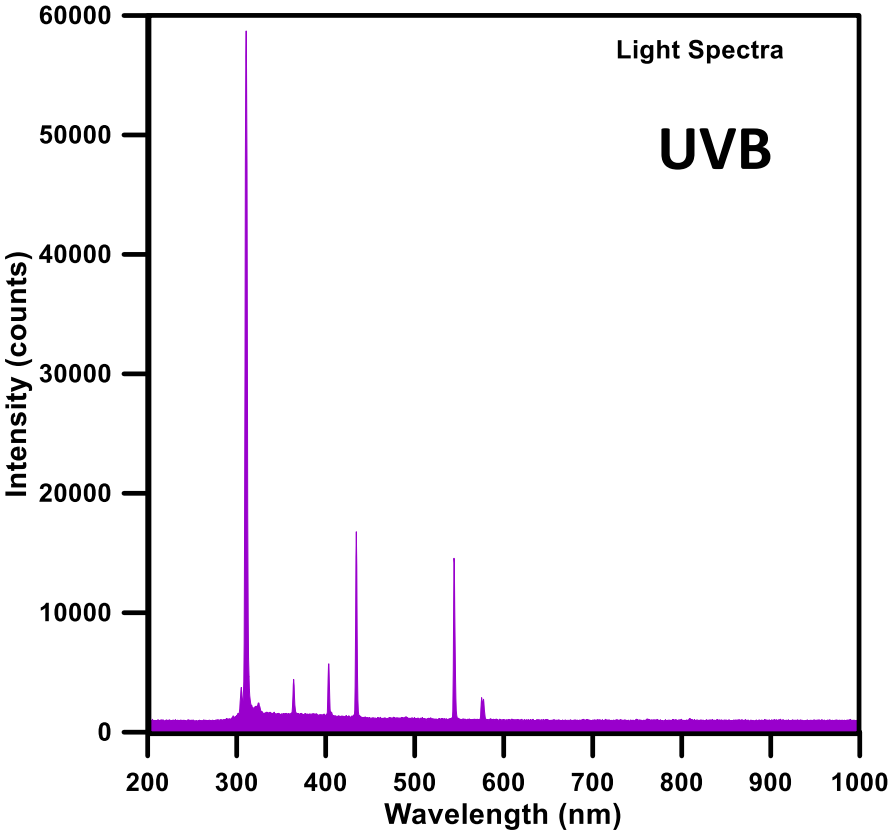

Figure S3. Light spectra for UVA lamps

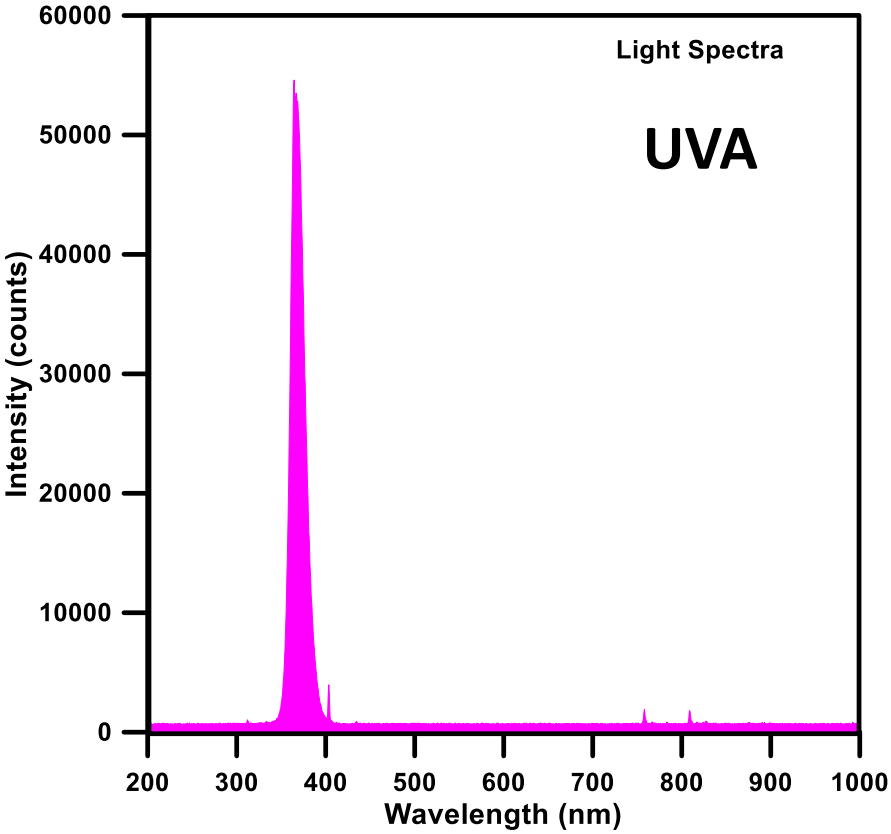

Figure S4. PMS consumption during different experiments at single, double and triple factor activation. . [Fe(VI)]= 1 mg L^{-1}; [PMS]= 5 mg L^{-1} and irradiation at 550 W m^{-2}.

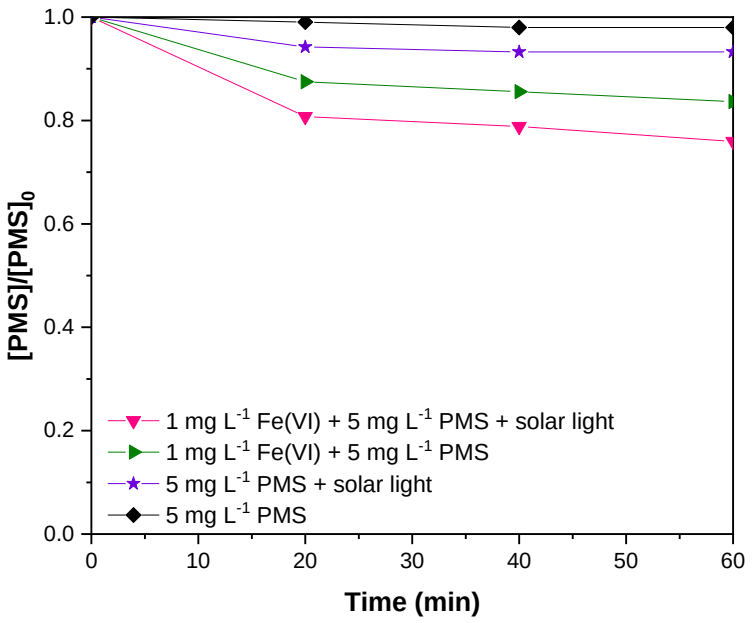

Figure S5. Scavenger tests: Three-factor inactivation process (Fe(VI), PMS and solar light), radical scavenging experiments and tests 50% D_2O in water. [Fe(VI)]= 1 mg L^{-1}; [PMS]= 5 mg L^{-1} and irradiation at 550 W m^{-2}; [tBuOH]= [MeOH]= 10 or 100 mM

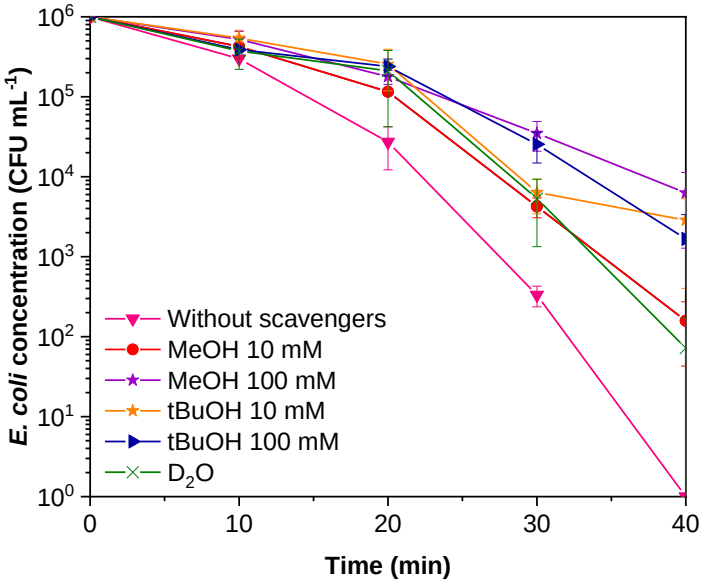

Table S1. Observed kinetic constants fitted by pseudo-first order kinetic by different inactivation curves of *E.coli* K12. [Fe(VI)]= 1 mg L^{-1}; [PMS]= 5 mg L^{-1}, solar irradiance: 550 W m^{-2}, T= 35 ºC; pH= 6.5.

Experimental conditions	**kobs (min^{-1})**	**R^2**
0.5 mg L^{-1} Fe(VI)	0.01	0.98
1 mg L^{-1} Fe(VI)	0.02	0.99
5 mg L^{-1} Fe(VI)	0.02	0.79
0.5 mg L^{-1} Fe(VI) + solar light	0.13	0.94
1 mg L^{-1} Fe(VI) + solar light	0.13	0.87
5 mg L^{-1} Fe(VI) + solar light	0.06	0.99
Solar light	0.10	0.97
10 mg L^{-1} PMS	0.07	0.97
5 mg L^{-1} PMS	0.01	0.47
5 mg L^{-1} PMS + solar light	0.15	0.98
10 mg L^{-1} PMS + solar light	0.16	0.97
1 mg L^{-1} Fe(VI) + 5 mg L^{-1} PMS	0.01	0.61
1 mg L^{-1} Fe(VI) + 5 mg L^{-1} PMS + solar light	0.34	0.91
1 mg L^{-1} Fe(VI) + 5 mg L^{-1} PMS + UVA	0.14	0.98
1 mg L^{-1} Fe(VI) + 5 mg L^{-1} PMS + UVB	0.03	0.58

Table S2. Observed kinetic constants fitted by pseudo-first order kinetic by different degradation curves of SMX in the Fe(VI)/PMS/solar light process. [Fe(VI)]= 1 mg L^{-1}; [PMS]= 5 mg L^{-1}, solar irradiance: 550 W m^{-2}, T= 35 ºC; pH= 6.5.

Experimental conditions	**kobs (min^{-1})**	**R^2**
1 mg L^{-1} Fe(VI)	0.001	0.65
Solar light	0.002	1
5 mg L^{-1} PMS	0.002	0.98
1 mg L^{-1} Fe(VI) + 5 mg L^{-1} PMS + solar light	0.02	0.98

Table S3. Observed kinetic constants fitted by pseudo-first order kinetic by different degradation curves of *E. coli* K12, *B. subtilis* and *R. Planticola* in the Fe(VI)/PMS/solar light process. [Fe(VI)]= 1 mg L^{-1}; [PMS]= 5 mg L^{-1}, solar irradiance: 550 W m^{-2}, T= 35 ºC; pH= 6.5.

Experimental conditions	**kobs (min^{-1})**	**R^2**
E. coli K12	0.34	0.91
B. subtilis	1.16	1.00
R. planticola	0.48	1.00